An Application of a Proposed Airdrop Planning System

by

Lucas Jonathan Fortier

B.S., Aerospace Engineering, Georgia Institute of Technology, 2002

SUBMITTED TO THE DEPARTMENT OF AERONAUTICS AND ASTRONAUTICS
IN PARTIAL FULFILLMENT OF THE REQUIREMENTS FOR THE DEGREE OF

MASTER OF SCIENCE
IN AERONAUTICS AND ASTRONAUTICS

AT THE

MASSACHUSETTS INSTITUTE OF TECHNOLOGY
JUNE 2004

Signature of Author_____
Department of Aeronautics and Astronautics

Certified by_____
Sean George
Charles Stark Draper Laboratory
Technical Supervisor

Certified by_____
Dr. Brent Appleby
Lecturer
Informational and Control Engineering Laboratory
Massachusetts Institute of Technology
Thesis Supervisor

Accepted by_____
Dr. Edward M. Greitzer
H. N. Slater Professor of Aeronautics and Astronautics
Chair, Committee on Graduate Studies

[This page intentionally left blank]

An Application of a Proposed Airdrop Planning System

by

Lucas Jonathan Fortier

Submitted to the Department of Aeronautics and Astronautics on
May 14, 2004, in partial fulfillment of the requirements for the
Degree of Master of Science in Aeronautics and Astronautics

ABSTRACT

The United States military has always had an increasing need for more accurate airdrops, whether the drops are being implemented for various special operations missions, or for basic humanitarian relief. Improving the delivery accuracy of airdrops will result in numerous benefits. In attempting to improve airdrop accuracy, it is helpful to know what errors will arise throughout the course of a drop. This information is effective in revealing to the airdrop personnel what steps can be taken to improve the airdrop, as well as what the expected landing accuracy of the airdrop will be. This research converges on tools to assist in the estimation and improvement of airdrop landing errors.

Wind estimation was studied to better understand the landing errors that stem from different wind prediction methods, as well as from onboard wind measurement systems. Other uncertainties, throughout each phase of an airdrop, are also known to produce landing errors, such as uncertainties in release conditions and parachute dynamics. These errors were implemented in airdrop simulations, for both unguided air release planning systems and guided airdrop systems, to determine the effects of these uncertainties on landing error.

Error in wind estimation was found to be the largest source of error in the airdrop simulations. Guided systems were hypothesized to have much smaller landing errors than the unguided systems, and that hypothesis was confirmed in this study. One major benefit of using guidance was the ability to implement onboard wind measurement systems. Using the data from the simulation results, this information was combined to produce an airdrop planning aid to assist airdrop personnel in their aerial deliveries. While the tool developed in this study is not a complete product, it represents a template on which to base further airdrop planning aids.

Technical Supervisor: Sean George
Title: Laboratory Technical Staff

Thesis Supervisor: Dr. Brent Appleby
Title: Lecturer, Informational and Control Engineering Laboratory

[This page intentionally left blank]

Acknowledgments

I would like to sincerely thank the Charles Stark Draper Laboratory for providing me with the wonderful opportunity to pursue an advanced degree at MIT. I am especially grateful to my project supervisors, Dr. Brent Appleby, thesis supervisor, and Sean George, technical supervisor, for their supportive assistance in my research.

I would also like to thank Roberto Pileggi, Tom Fill, Philip Hattis, and Professor Wallace VanderVelde for their assistance with this project

This material is based upon work supported by the Army Contracting Agency - Yuma, under contracts DABJ49-03-C-0013, W9124-04-C-0018 and DATM0-02-C-0039. Any opinions, findings and conclusions or recommendations expressed in this material are those of the author(s) and do not necessarily reflect the views of the Army Contracting Agency-Yuma.

This material is also based upon work supported by Draper Internal Research and Development. Publication of this thesis does not constitute approval by Draper or the sponsoring agency of the findings or conclusions contained herein. It is published for the exchange and stimulation of ideas.

[This page intentionally left blank]

Table of Contents

List of Tables

List of Figures

Chapter 1
Introduction

1.1 Project Background

The United States military has always had an increasing need for more accurate airdrops, whether the drops are being implemented for various special operations missions, or for basic humanitarian relief. Improving the delivery accuracy of airdrops will result in numerous benefits. A key benefit will be reduced losses of airdropped supplies by facilitating the placement of these supplies where they are needed. Accounts of airdrops from the Vietnam War, for example, describe situations where airdropped supplies to the French army missed their target and ended up with the enemy. Airdrops can also be made safer for the aircrews by allowing airdrops to be released from higher altitudes while still enabling the dropped supplies to reach the target [1]. Planes flying in enemy territory are at higher risk to anti-aircraft weapons at lower altitudes. Improving accuracy will also allow airdrops to be performed in more places than the current technologies permit, as drop zones must be large enough to account for any errors that might arise throughout the course of the drop [2]. Attempting to place airdropped payloads into too small of an area could not only result in loss or damage to the payload, but could incur damage on surrounding buildings, structures, and people.

Conventional military airdrops consist of 'round' unguided parachute systems with no ability to be steered once in the air. Figure 1.1 shows a picture of conventional canopies.

Figure 1.1. G-12s Airdropped from a C-130

Several factors are helpful in improving the accuracy of these conventional airdrops. Enhancing the determination of the optimal release point from the release conditions and the estimated wind patterns is one objective for improving accuracy. Improving the wind sensing ability is also known to be an effective technique in improving airdrop accuracy, as the better the wind conditions are known, the better the release point can be calculated. Using a guided delivery system is another means of improving airdrop accuracy by allowing the system to steer itself towards the target throughout the descent [3]. Figure 1.2 displays a parafoil that a guided system can control.

Figure 1.2. Parafoil in Flight

Draper Laboratory has been developing technologies to improve accuracy of both unguided and guided airdrop systems. A guided system known as PGAS, or Precision Guided Airdrop System, was developed to provide accurate delivery within 100 meters of the target [2]. The parafoil actually achieved landing accuracies of about 35 meters, with much of the landing attributed to uncertainties in GPS altitude [2]. A ballistic system known as WindPADS, or Wind-Profile Precision Aerial Delivery System, was also developed to improve the delivery accuracy of 1000-2200 pound payloads via high altitude airdrop. WindPADS combines an onboard airdrop planner with a wind and density field estimator to enable more accurate airdrops [1]. Draper followed this with the development of a guided airdrop planning system, which combined the guidance ability from PGAS with the airdrop planning ability from WindPADS.

This project attempts to continue the pursuit of improving airdrop accuracy. The driving sources of error are identified for various airdrop situations. These driving sources of error should be given more importance when seeking methods to reduce landing errors. Using the error analysis, a tool is developed to assist in the planning phase of an airdrop. This planning tool is able to predict the landing accuracy that can be attained for a given system. The tool is also able to determine what types of adjustments can be made to the airdrop situation to achieve a desired accuracy. The tool developed in this study is not a generic product, as it is only representative of the systems used in this study. However, the methodology behind the planning tool represents a template for developing a practical airdrop planning aid for a wide range of airdrop systems.

1.2 Simulation Overviews

In this study, two separate simulations were utilized to simulate actual airdrops. For unguided airdrop analysis, a simulation from the WindPADS program was used known as PADS, or Precision Aerial Delivery System. The PADS simulation handles three degree-of-freedom dynamics models, along with experimental look-up tables, of unguided, ballistic airdrop systems. All phases of airdrop flight are analyzed, including:

extraction, stabilization, steady-state descent, and landing. PADS can handle a variety of different aircraft, parachutes, and payloads, among other variable parameters. Also included in the software is the capability for Monte Carlo simulation, which is useful in probabilistic error analysis.

For guided airdrop analysis, the simulation from the PGAS program was used. The simulation utilizes representations of parachute dynamics, navigation sensors, expected environment, and onboard wind measurement systems. The type of parafoil used in this simulation is known as the "Wedge 3," which was developed by the NASA Dryden Flight Research Center (DFRC). The parafoil has a surface area of 88 square feet [2]. Although PGAS has the ability to handle various types and sizes of parafoils, only one kind will be used to analyze the performance of guided airdrop systems. Like the PADS simulation, the PGAS software is capable of performing Monte Carlo simulations.

1.3 Thesis Outline

The primary goal of this thesis is to develop a tool to assist in the planning phase of an airdrop. Wind conditions and wind knowledge have been known to be a major factor in the accuracy of airdrops; therefore wind prediction errors are analyzed and modeled, along with methods for developing realistic wind conditions. Both unguided and guided systems are simulated to determine the driving errors for each respective system. Total expected landing errors for these systems are also determined. These findings are then brought together to develop the tool to assist in airdrop planning.

Chapter Two describes several wind prediction methods that are used throughout this study. The errors that these wind prediction methods provide are determined and modeled. Techniques for generating realistic wind conditions are discussed, along with algorithms to effectively integrate onboard wind measurement systems into the airdrop system's wind prediction.

Chapter Three analyzes the errors present in unguided air release planning systems. Individual error sources, including errors in release conditions, parachute dynamics, and wind conditions, are examined to determine the driving error sources inherent in the system. Expected landing errors are determined for various scenarios, and methods for error reduction are discussed.

Chapter Four analyzes the errors present in guided airdrop systems. Similar to the study of unguided systems in Chapter Three, expected landing errors are determined for various scenarios. Different methods of pre-drop wind knowledge are examined, as well as methods of achieving wind knowledge during the descent.

Chapter Five combines the results from Chapters Three and Four and develops a tool to assist in the planning phase of the airdrop. This tool does not represent a generic product that can be currently used for any airdrop system, but rather a template to develop a practical airdrop planning aid. Examples of the use of this planning tool are shown to display its ability to determine what kind of accuracy is attainable with a given system, and to determine what types of adjustments can be made to the airdrop situation to achieve a desired accuracy.

Chapter Six presents the conclusions of this research effort and makes recommendations for further study in the area of airdrop accuracy.

Chapter 2
Wind Characteristics

2.1 Introduction

Airdrop systems are never completely accurate. There are many factors that affect the landing location of an airdrop, chief among them being the wind conditions at the time of the drop. It is important to understand the behavior and uncertainty statistics of wind when making wind predictions, as wind prediction error can be one of the most significant sources of landing error. This chapter is devoted to modeling wind prediction errors to assess the impact that wind error has on airdrop accuracy.

Methods for developing wind predictions are discussed below. Along with the different wind prediction methods, there are different techniques for describing the wind prediction errors to assess the impact that wind has on airdrop accuracy. Some of these methods are also discussed below, and one method is chosen to be the technique to be used throughout the remainder of this study.

The wind samples used in this study for purposes of wind modeling and wind error prediction are taken from Yuma, Arizona. This is mainly because a large sampling of wind from Yuma was readily available. Therefore, most of the succeeding wind data will be specific to Yuma; however, the statistical methods used here, as well as the general insights gained from this research can be applied to wind analysis anywhere.

2.2 Wind Prediction Methods

There are numerous methods to develop wind predictions. The most basic method, and least accurate, is to use general wind statistics for the area where the airdrops are to be performed. This historical data is usually in the form of monthly or daily averages of wind speeds at various altitudes.

Weather forecasting is a more accurate predictor of wind than the general wind statistics. Forecasts can be made at any time preceding an airdrop, with the more accurate forecasts using wind data closer to the drop. There are many methods to enhance forecasts, including the use of balloons and/or dropsondes to provide updated wind samples for the forecast.

The most accurate wind prediction method is onboard sampling. This is only effective for guided airdrop systems, as only the guided system can alter its course depending on the updated wind knowledge after it is dropped. One type of onboard sampling is to measure the wind at the current altitude, and estimate the winds at lower altitudes using the current measurement. Another type of onboard sampling is to measure the winds at lower altitudes and use that measurement to estimate the winds at other altitudes. This can be done with a LIDAR system, among others, and is a powerful method for measuring the wind field that the system will encounter.

2.2.1 General Wind Statistics

There has been a joint effort between the United States Navy and the Department of Commerce to produce general wind statistics for various locations around the world. One of those locations is Yuma, Arizona. For eight years (1980-1987), wind measurements were taken twice daily at various altitudes by use of radiosonde launches, aircrafts, and satellites. Although differences were noticed between winds during different months, these differences were small. It was therefore acceptable to generalize the wind patterns

over the entire year, rather than month-to-month. Table 2.1, shown here, displays the general wind statistics for Yuma, Arizona at given altitudes.

Table 2.1. General Wind Statistics for Yuma, Arizona

	Average (ft/s)		Standard Deviation (ft/s)	
Altitude (ft)	**North**	**East**	**North**	**East**
5,000	1.4	6.9	9.0	7.0
10,000	1.1	11.7	18.8	19.3
19,000	-0.7	28.1	30.0	30.4
25,000	-0.8	38.6	36.8	37.0

It can be seen in Table 2.1 that the average North winds are much smaller than the average East winds. The average North winds are around zero ft/s. The East winds, however, have a non-zero average that increases with altitude. Using a least-squares method for a linear curve-fit, one can derive a function for the averages and standard deviations of North and East winds as a function of altitude. The linear approximations (in the form $y = mx + b$) are shown below in Table 2.2.

Table 2.2. General Wind Statistics Approximation Parameters

Parameter	**North Mean**	**North St. Dev.**	**East Mean**	**East St. Dev.**
Slope (s^{-1})	-0.0001	0.0014	0.0016	0.0014
Intercept (ft/s)	2.09	3.58	-2.71	2.07

These approximations will be used later when analyzing airdrop systems under specific wind conditions.

2.2.2 Wind Forecasting Statistics

Unlike the general wind statistics, the forecasted wind files are all available in raw data form. In other words, the entire forecasted wind profiles, along with the entire corresponding measured wind profiles are available. All the wind files used in this forecasting analysis are taken from tests that the NWV team has performed, and the wind prediction method of choice was a forecast combining Air Force Weather Agency (AFWA) data along with wind measurements made by balloons. This data is the only data readily available to the NWV team for analyzing wind prediction methods and developing wind error statistics. If data from other wind prediction methods are available, similar approaches as shown in this chapter can be used to develop alternative wind error statistics that are more appropriate to the desired wind prediction method.

When the NWV team tests their unguided air release planning system, wind readings are recorded for each drop. About 15-30 minutes before each drop, a balloon is sent up to measure the wind velocity at numerous altitudes using GPS. Then, a meteorological expert working with the NWV team combines the balloon data with a weather forecast to project the winds at a later time. Three-dimensional wind fields are provided by the AFWA. This information is then assimilated with the balloon data to forecast the winds in the future. This projection is known as the predicted wind. It is with this wind prediction that the NWV team calculates the aerial release point for the payload.

When the airplane reaches the release point, the parachute is deployed out of the back of the plane. A radar apparatus on the payload of the parachute tracks its motion through its descent. The NWV team then takes that radar data and extracts what is called a truth wind. This is the actual wind that the parachute experienced during the drop.

Almost immediately after the parachute is released out of the plane, a second chute, known as a windpack, is released. The windpack is a wind measurement device that also provides a truth wind as it descends towards the ground by using a GPS receiver to record its ground track. It provides similar data to the radar wind track, with small differences

due to the different trajectory and time lapse. In comparing the predicted and the truth winds, files were provided by the NWV team. Twelve balloon predictions along with the corresponding windpack truth files, and twenty balloon predictions along with the corresponding radar truth files, provide a total of 32 prediction and truth comparisons.

2.3 Error Description Methods

2.3.1 Errors in the North and East Directions

In order to determine the most appropriate system for describing the statistics of wind, it is first necessary to analyze past data. The first method considered for describing the wind prediction errors is to compare the wind velocity magnitudes in the North and East directions between the predicted and the truth winds. These are the directions used in the source files. Since North and East are arbitrary directions, their statistics can be combined to compute the statistical parameters. Errors were computed at specific altitudes, for all compatible predicted and truth files. A histogram of the errors is shown below in Figure 2.1. This histogram shows that the North and East wind errors appear to take on a Gaussian distribution with approximately zero mean.

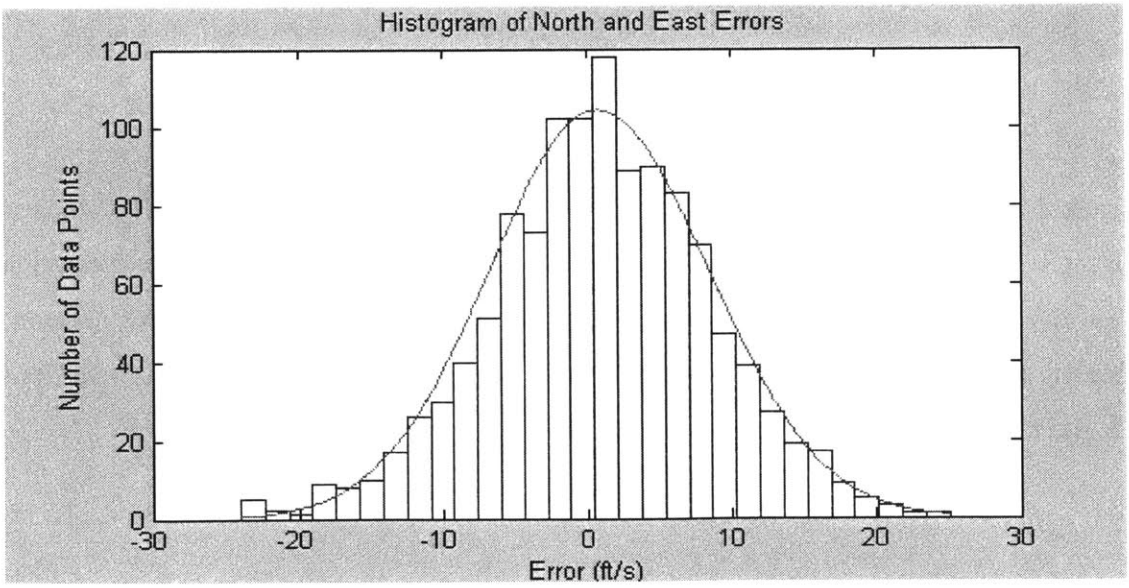

Figure 2.1. Histogram of North and East Errors

Another approach to the North and East error analysis is to normalize the wind velocity errors by the predicted wind magnitude to give a fractional error value. Normalization takes into account the magnitude of the predicted wind when describing the statistics. As in the previous figure, errors were computed at specific altitudes for all compatible predicted and truth files. A histogram of the normalized errors is shown below in Figure 2.2.

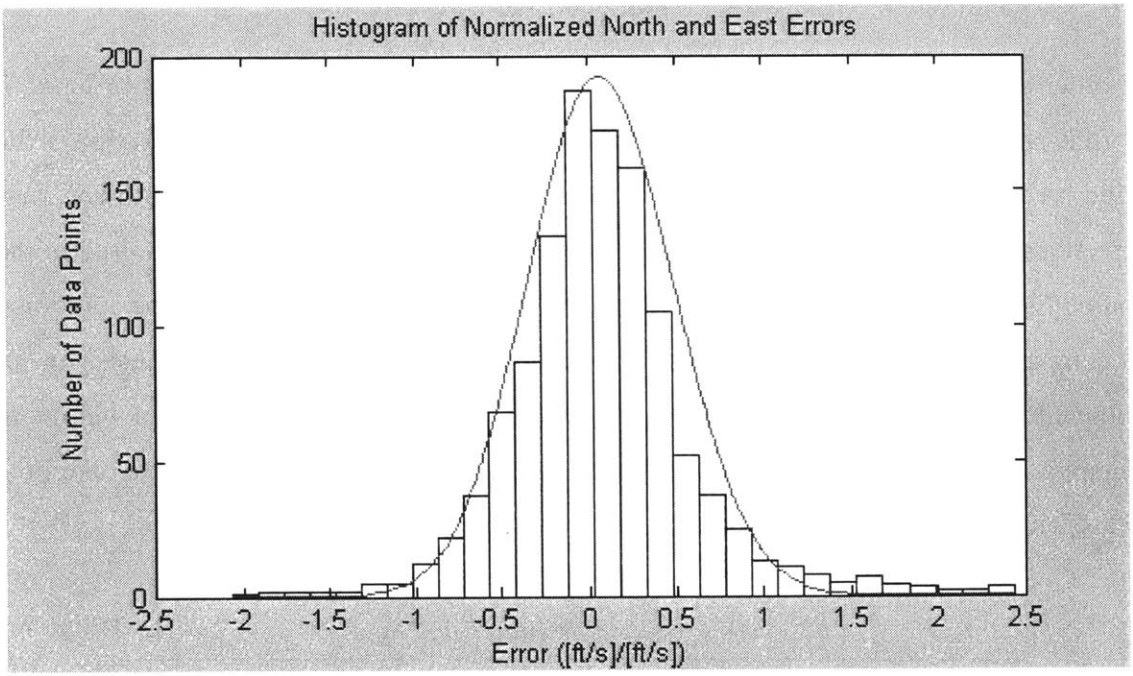

Figure 2.2. Histogram of Normalized North and East Errors

Figure 2.2 reveals that the normalized errors are also Gaussian distributed. The statistics for the original and normalized errors are shown below in Table 2.3. Extreme data points were discarded before the subsequent values were calculated to reduce any abnormal skewing that might result from extreme values. The resulting values produce close-fits to the given data. As expected, the means are close to zero.

Table 2.3. Statistical Parameters for East and North Errors

	Original Errors	**Normalized Errors**
Mean	0.84 ft/s	0.072
Standard Deviation	7.15 ft/s	0.52

2.3.2 Errors in Magnitude and Azimuth

The second method of describing the errors is to compare the absolute magnitude and the azimuth angle for the predicted and the truth winds. As with the North and East errors, histograms were developed to illustrate the distributions. Figure 2.3, shown below, displays that the magnitude errors appear to take on a Gaussian distribution.

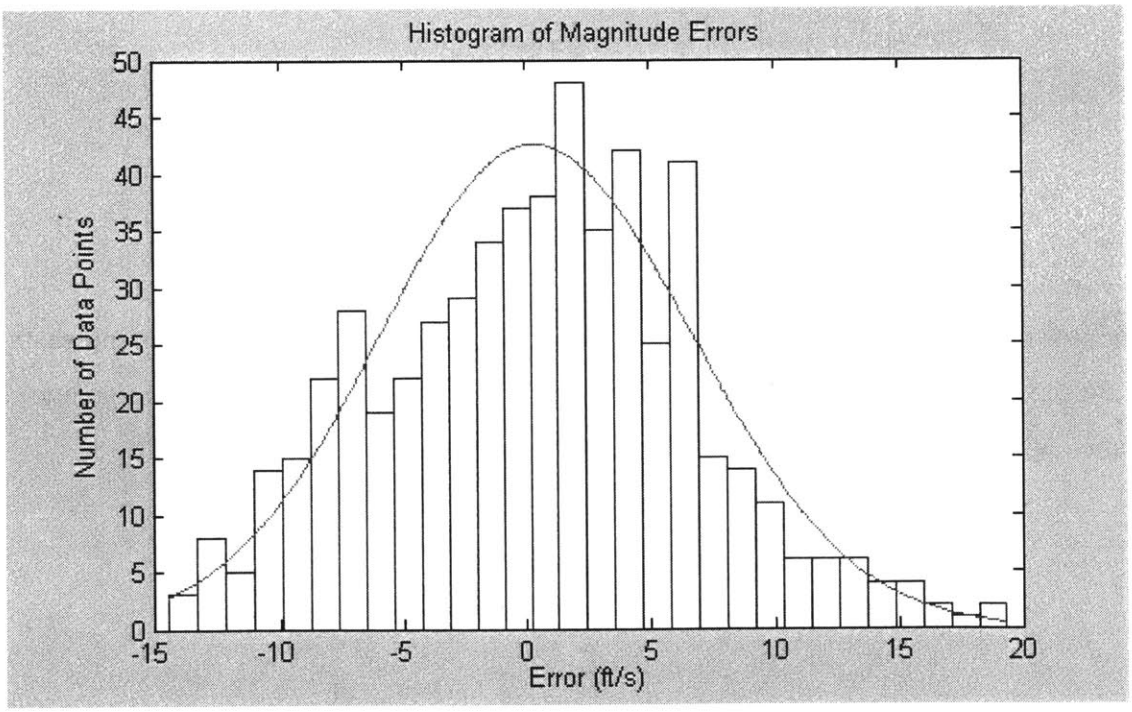

Figure 2.3. Histogram of Wind Magnitude Errors

The magnitude differences were normalized with respect to the predicted wind magnitude and the histogram is shown below in Figure 2.4. This distribution also appears Gaussian, but it is improper to describe the normalized magnitude differences as Gaussian due to the fact that it is impossible to have a value less than –1.

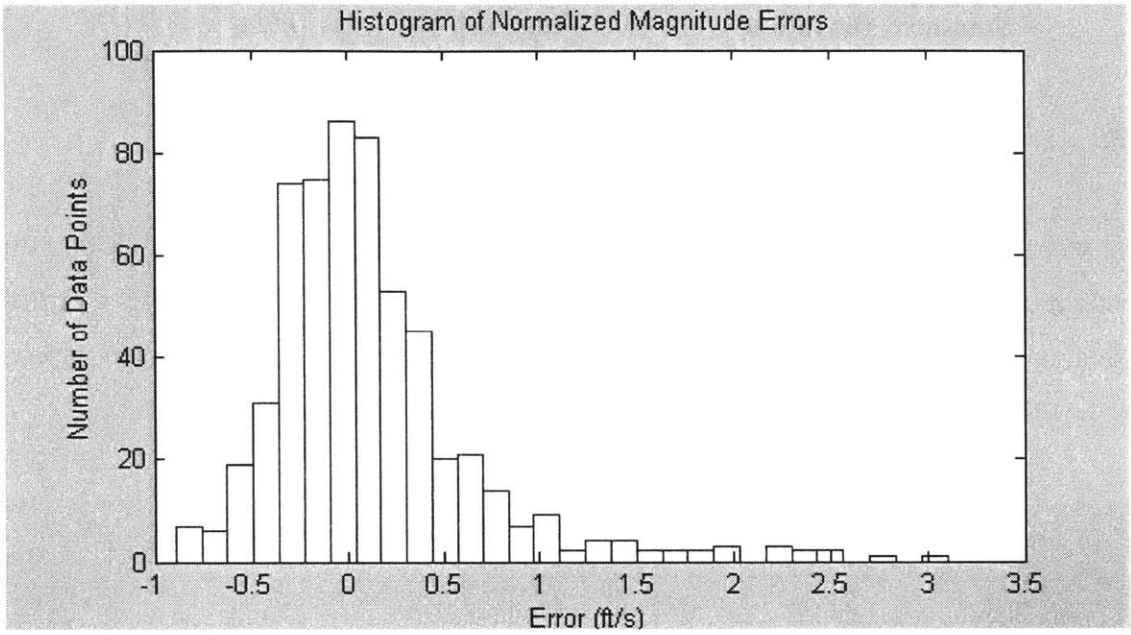

Figure 2.4. Histogram of Normalized Magnitude Errors

The azimuth angle is the angle with respect to due north, with positive angles increasing in the clockwise direction. Similar to the magnitude errors, the azimuth errors also appear Gaussian. Figure 2.5, shown below, displays the azimuth errors histogram.

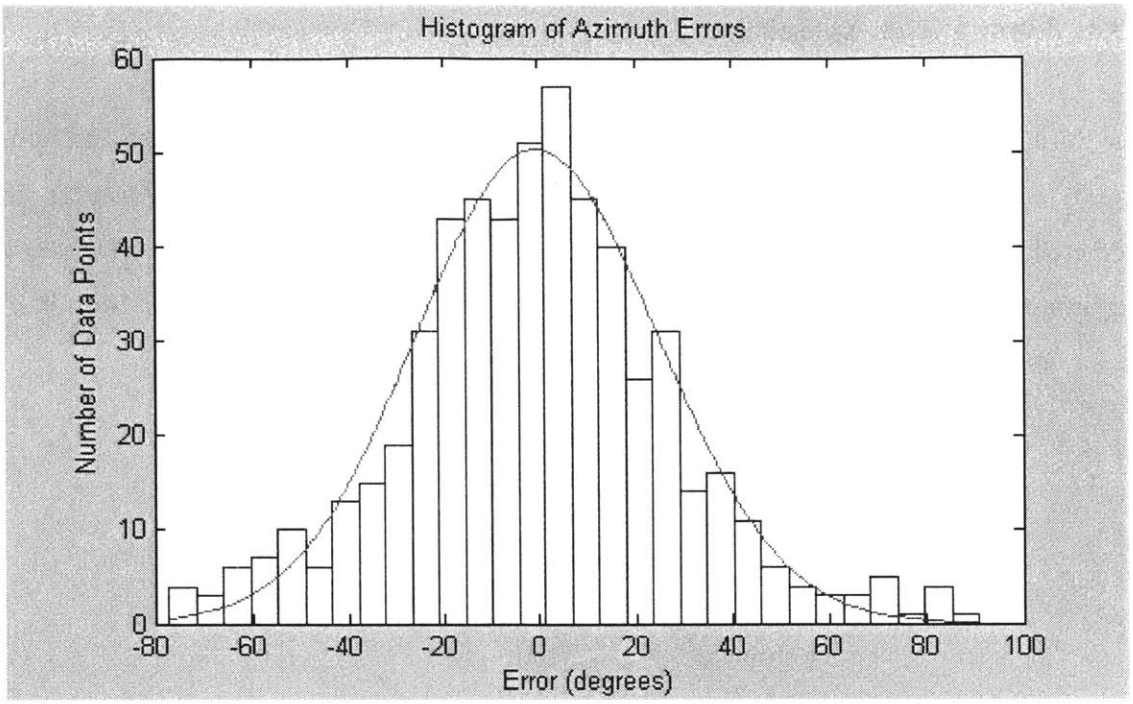

Figure 2.5. Histogram of Azimuth Errors

The statistics for the magnitude (original and normalized) and azimuth errors are shown below in Table 2.4. Extreme data points were discarded and the resulting values produce close-fits to the given data. Again, they are all approximately zero mean. Due to the fact that there is no upper bound on the magnitude error, while there is a lower bound, the mean is slightly greater than zero.

Table 2.4. Statistical Parameters for Magnitude and Azimuth Errors

	Original Magnitude Errors	**Normalized Magnitude Errors**	**Azimuth Errors**
Mean	0.78 ft/s	0.12	-0.17 deg
Standard Deviation	8.33 ft/s	0.54	41.36 deg

2.3.3 Error Vector Approach

The third and final method for describing errors between the predicted and the truth wind files is to calculate the error vector. The error vector is found from subtracting the predicted wind vector from the truth wind vector. In visual reasoning, it is the vector beginning at the end of the predicted wind vector, and ending at the end of the truth wind vector, as shown here.

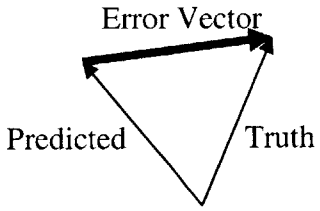

Figure 2.6. Error Vector Drawing

The error vector magnitude can never take a value below zero; therefore it isn't completely accurate to describe the magnitude data as Gaussian. Figure 2.7, shown below, shows the histogram of the error vector magnitudes. Although the data is not Gaussian, it still resembles an exponential function. More specifically, it bears a resemblance to a Rayleigh density function. A Rayleigh density function transpires when two orthogonal, zero mean, Gaussian components (in this case, North and East) are merged to form a magnitude and direction. The magnitude is then Rayleigh distributed.

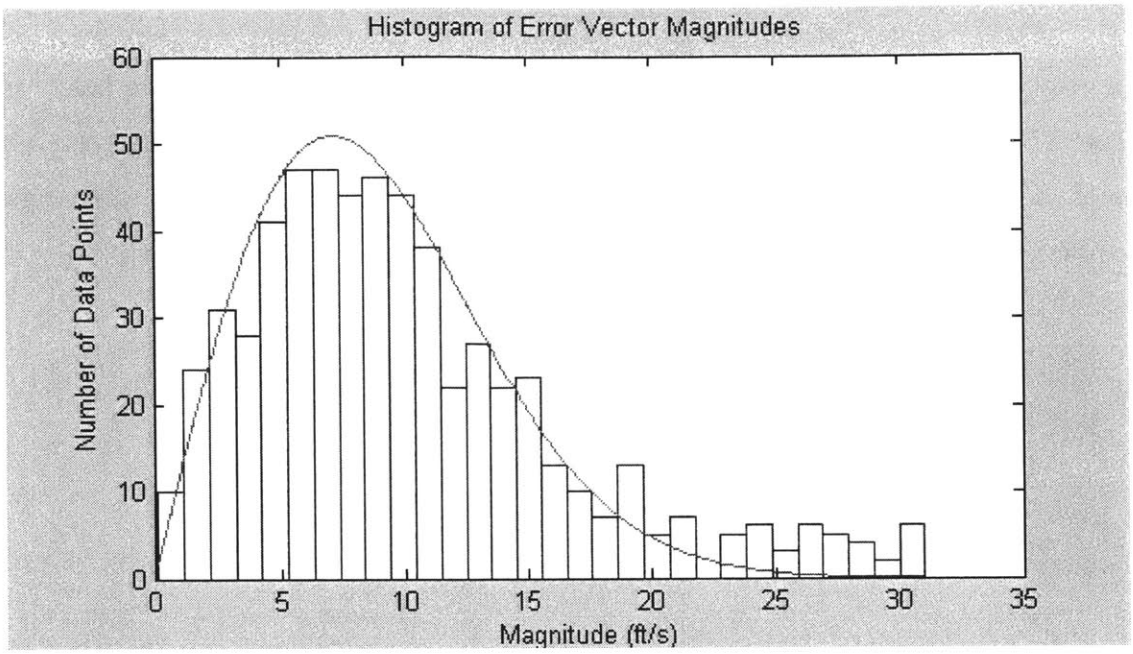

Figure 2.7. Histogram of Error Vector Magnitudes

The error vector magnitudes were also normalized with their respective predicted wind magnitudes. Figure 2.8, shown below, displays the normalized magnitudes in a histogram. This shows an even greater resemblance to a Rayleigh distribution.

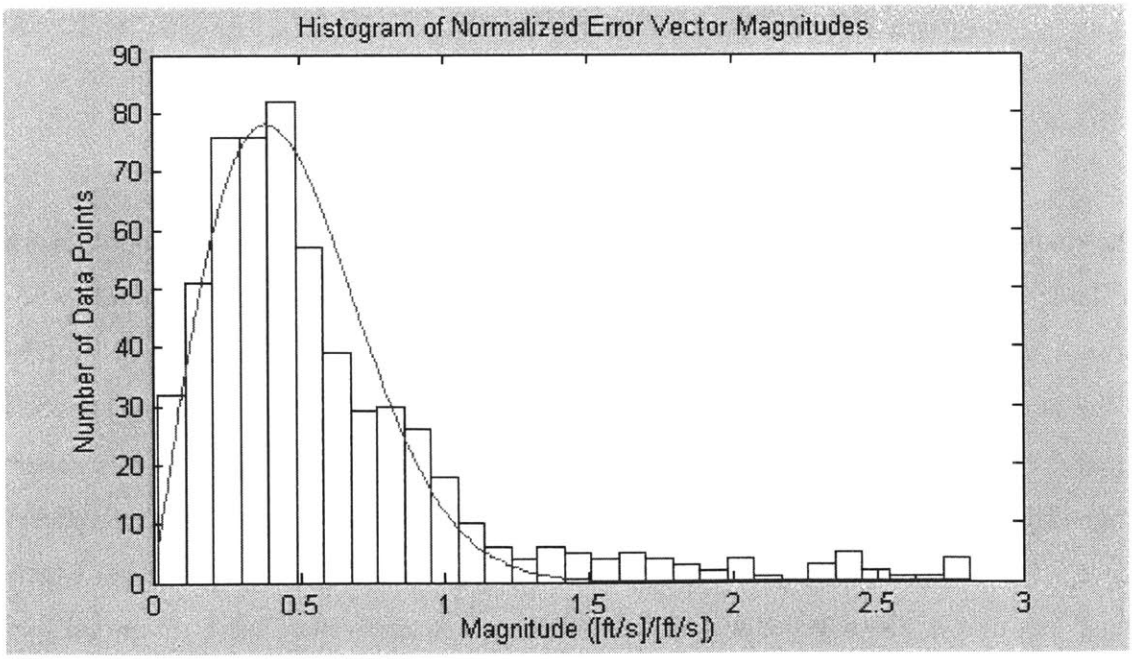

Figure 2.8. Histogram of Normalized Error Vector Magnitudes

The error vector azimuth angles were computed and their histogram is shown below in Figure 2.9. There is no apparent pattern to the distribution, so it is inferred that the error vector azimuth angles are uniformly distributed. This is expected, as the angle distribution that complements a Rayleigh distributed random variable is uniform.

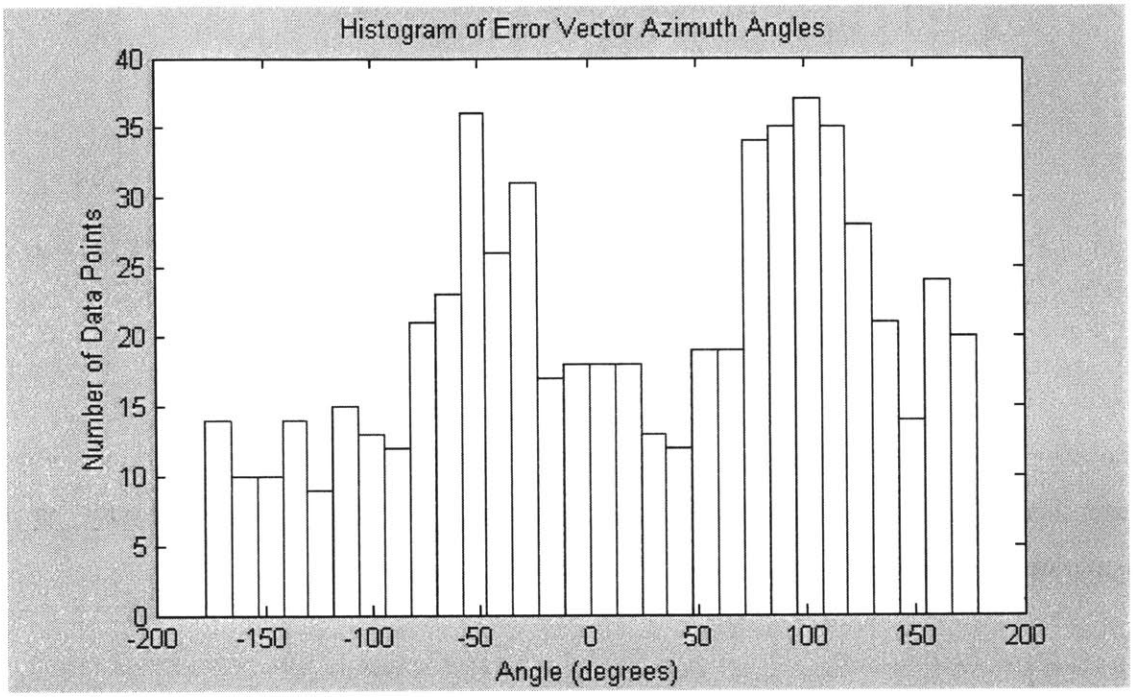

Figure 2.9. Histogram of Error Vector Azimuth Angles

The statistics for the error vector magnitudes (original and normalized) are shown below in Table 2.5. Again, extreme values were discarded, and the results were found to be a close fit to the given data. The only parameter needed to describe a Rayleigh distribution is the mode (or peak value). One property of a Rayleigh distribution is that the mode is equal to the standard deviation of the orthogonal components with which it was derived from. The standard deviations in Table 2.3 are approximately equal to the modes in Table 2.5, thus adhering to this property of a Rayleigh distribution. They are not exactly equal, but that is just due to the fact that different extreme values were discarded from each data set before the calculations were performed.

Table 2.5. Statistical Parameters for Error Vector Magnitudes

	Original Magnitude	Normalized Magnitude
Mode	8.4 ft/s	0.56

2.3.4 General Error Magnitudes

Three methods have been shown for describing the error between the predicted winds and the truth winds. These descriptions are completely independent of altitude. The only parameter that affects any of the error descriptions is the magnitude of the predicted wind. Analysis was performed to determine the effect of altitude on the statistical parameters of the errors. The results were inconclusive with the data available. Perhaps with more data, a pattern or trend in the error statistics can be observed as altitude increases or decreases. For now, the errors will be described without taking into account for altitude. In other words, the wind error standard deviation profiles will be assumed constant with respect to altitude.

For errors in the North and East directions, as well as the error vector approach, there is still the option of using normalized errors or non-normalized errors. Figure 2.10, shown below, displays the magnitudes of the north and east errors (absolute values of the errors) given a predicted wind magnitude. The data is grouped by the predicted wind magnitudes in intervals of 5 ft/s.

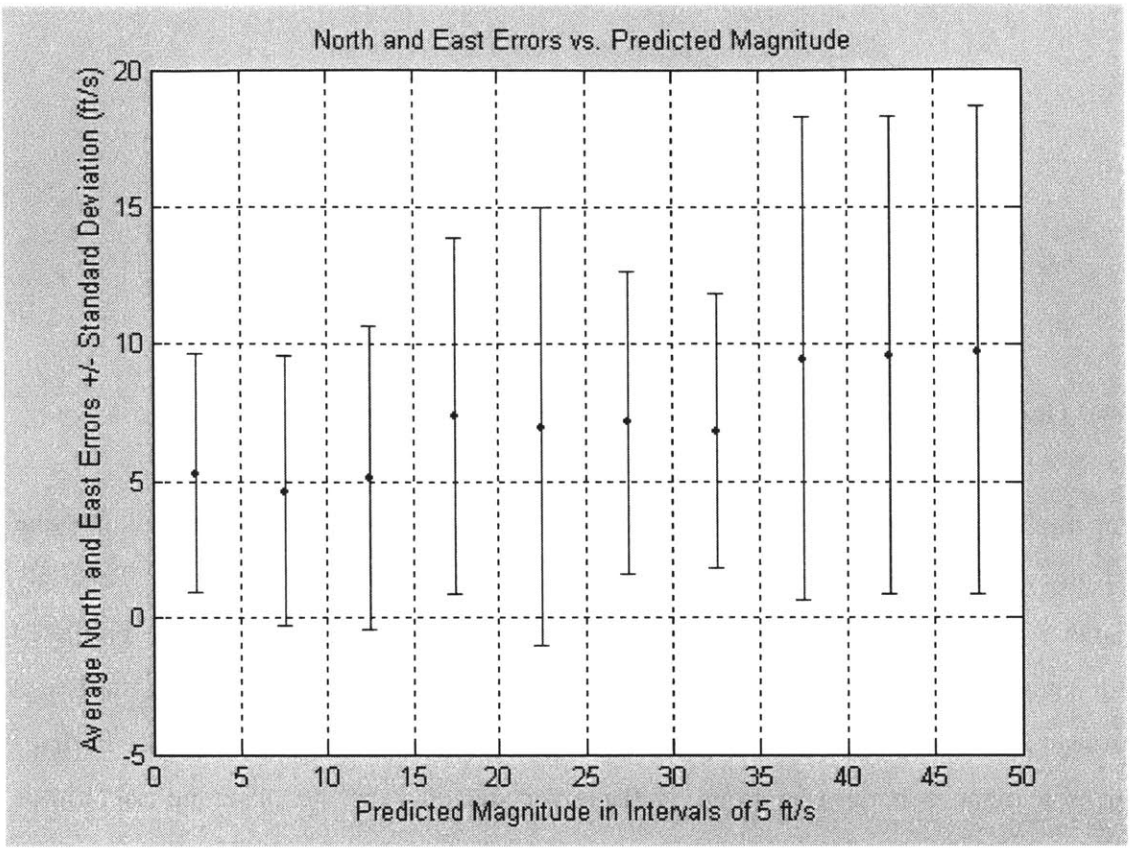

Figure 2.10. North and East Errors vs. Predicted Magnitude

From the graph in Figure 2.10, it can be seen that the average magnitude of the North and East errors slightly increases as the predicted wind magnitude increases. It also appears that the range of errors (characterized by the standard deviation) also tends to grow as the predicted magnitude grows. In spite of this, the data does not show increases that are significant enough to justify the use of normalized wind errors. In the first interval, where the predicted magnitudes are between zero and five ft/s, the average North and East error magnitude is more than 100% of the predicted magnitudes. In larger ranges, such as the 35-40 ft/s range, the average North and East error magnitude is closer to 25% of the predicted magnitudes.

Because of the inconsistency across the range of predicted magnitudes, it is not accurate to describe the North and East wind errors by use of a generic normalization distribution. If normalization of the errors were desired, it would be necessary to describe the

normalization distribution as a function of predicted magnitude. In Figure 2.10, it can be shown that a vertical range from approximately 2-9 ft/s can be placed across all the error bars. This range is sufficient enough to justify the use of using a generic non-normalized distribution to describe the errors across the entire range of predicted magnitudes.

2.4 Altitude Correlation

Once the general random statistics of individual wind errors are known, the next step is to determine the correlation with respect to altitude difference for the wind errors. For a given set of n data points, X, and a corresponding set of n data points, Y, the correlation between the two data sets is given by the following formula.

$$\rho = \frac{n \cdot \sum_i x_i \cdot y_i - \sum_i x_i \cdot \sum_i y_i}{\sqrt{n \cdot \sum_i x_i^2 - \left(\sum_i x_i\right)^2} \cdot \sqrt{n \cdot \sum_i y_i^2 - \left(\sum_i y_i\right)^2}} \tag{2.1}$$

This correlation equation was used to calculate the correlations of the wind errors with respect to the errors' altitude difference. Figures 2.11-2.14 show the correlation between the wind errors with respect to altitude difference. Figure 2.11 displays the correlations for the North and East errors. Figure 2.12 displays the correlations for the normalized North and East errors. Figure 2.13 displays the correlations for wind magnitude and azimuth errors. Figure 2.14 displays the correlations for the error vector magnitude and azimuth angles.

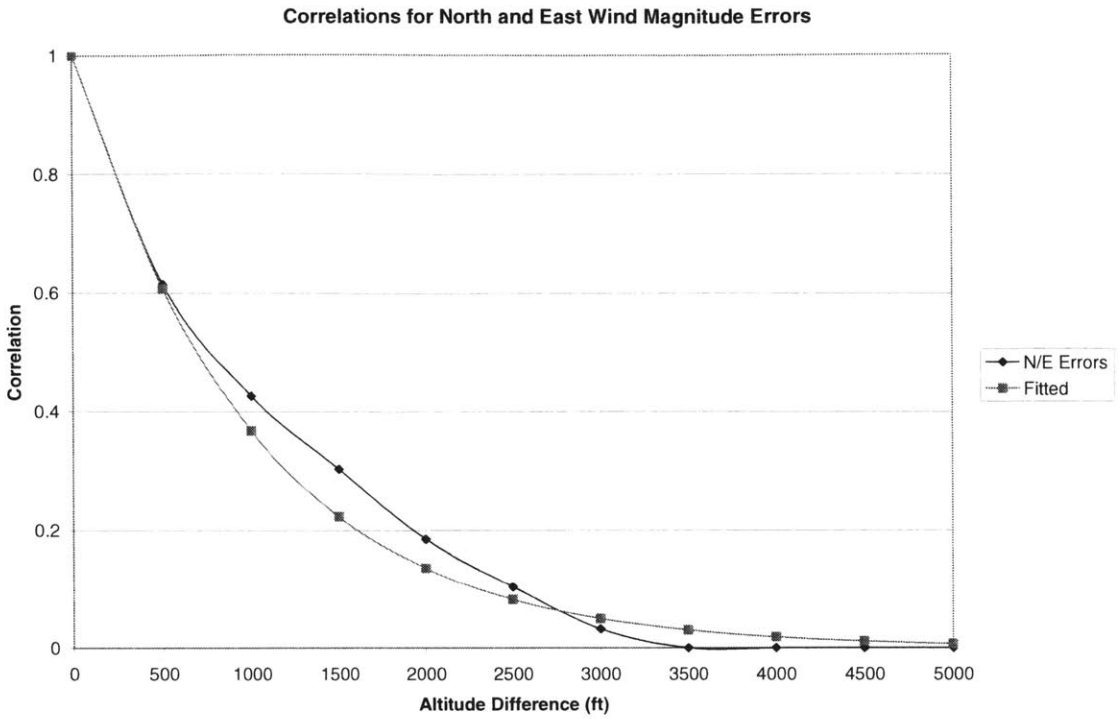

Figure 2.11. Correlations for North and East Wind Magnitude Errors

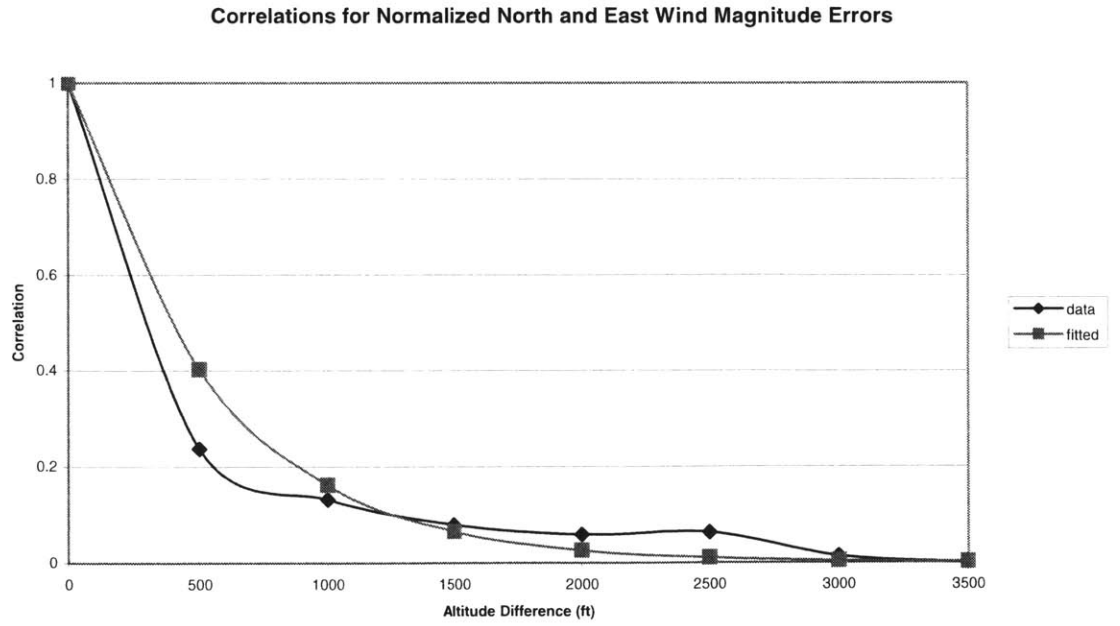

Figure 2.12. Correlations for Normalized North and East Wind Magnitude Errors

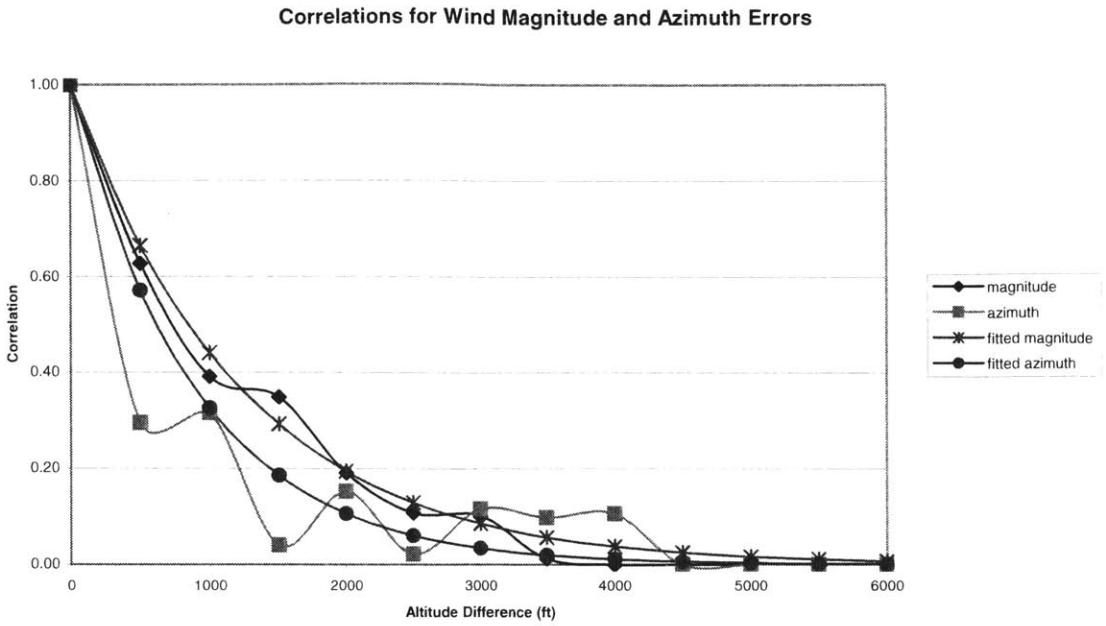

Figure 2.13. Correlations for Wind Magnitude and Azimuth Errors

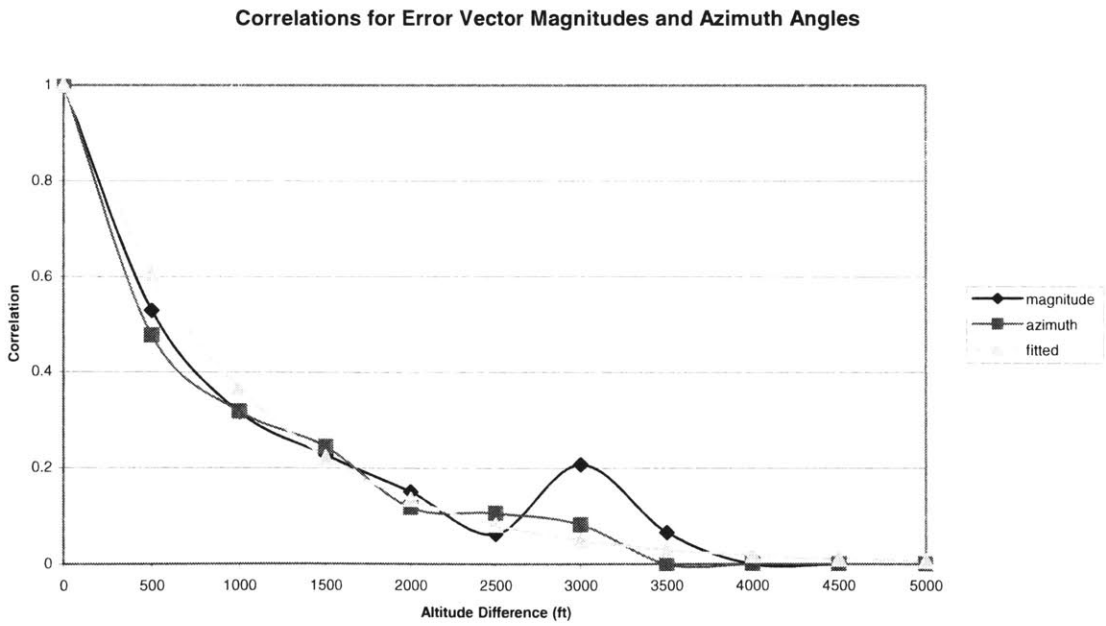

Figure 2.14. Correlations for Error Vector Magnitudes and Azimuth Angles

For each correlation plot, there is a generated exponential curve that fits the data. In the Global Reference Atmospheric Model (GRAM) initially developed by NASA in 1974, wind error correlations are assumed to be exponential of the form:

$$\rho = \exp(-\Delta h / \varepsilon) \tag{2.2}$$

where Δh is the altitude difference and ε, the correlation factor, is an empirical value that fits each specific type of data [4]. The values for ε that are used in Figures 2.11-2.14 to fit the correlation data are shown below in Table 2.6.

Table 2.6. Correlation Curve-Fitting Parameters

	ε (ft)
Figure 2.11	900
Figure 2.12	550
Figure 2.13 magnitude	1220
Figure 2.13 azimuth	890
Figure 2.14	1000

As with the uncorrelated error statistics, the correlation formulas do not depend on altitude. The correlation formulas only depend on the difference in altitude between the two points in question. This is not consistent with the GRAM model used by NASA. In GRAM, the empirical value, ε, is a function of altitude. The available data was analyzed to reveal how the correlation due to the difference in altitude changes with altitude. No conclusive findings were discovered. There did not appear to be any pattern or trend for any correlation values as the altitude range was changed. Therefore, in the analysis shown here, ε is a constant value throughout the range of altitudes. With more data, however, this result could be found to be inaccurate.

2.5 Generating Truth Wind Profiles

An important consequence to developing the statistics for the wind errors is the ability to generate simulated truth wind profiles based on predicted wind profiles for Monte Carlo performance analysis. The new truth wind profiles are developed from both the statistics for the individual predicted wind vectors, as well as the correlation between each predicted wind vector.

Three methods of describing winds errors were discussed; therefore it is left to the engineer which method they prefer when using the statistics to generate truth wind profiles. Method 1, errors in the North and East directions, is the simplest method due to the fact that the errors are zero mean and Gaussian. Since Method 1 is the simplest of the three methods, that will be the method implemented in the simulations throughout the project.

Method 2, errors in magnitude and azimuth, appears to be a straightforward method for generating truth winds. However, if the magnitude errors are classified as Gaussian, there is a chance that negative magnitudes will appear in the results, and a negative magnitude does not exist. That is why the normalized magnitude error can never be less than –1 (see Figure 2.4). Therefore, it is necessary to put a limit on the maximum negative error, and this causes difficulty when mathematically describing the statistics in order to generate truth winds.

Method 3, the error vector approach, is derived from Method 1. The magnitudes and azimuth angles for the error vectors are functions of the North and East errors, therefore the same results as Method 1 would be expected when generating truth wind profiles. Due to the fact that the error vector magnitudes are Rayleigh distributed makes the problem of generating correlated truth wind profiles much more difficult. Methods involving Inverse Discrete Fourier Transforms have been developed to solve this problem [5].

2.5.1 North and East Error Method of Truth Wind Generation

The North and East error method of truth wind generation for simulations was chosen due to the fact that the math involved is much simpler than the other methods. The North and East errors are assumed to be independent of each other, thus they can be handled separately. These errors are zero-mean and Gaussian distributed; therefore, it is helpful to develop a covariance matrix to generate sample error profiles. The following steps outline the means of calculating correlated sample wind errors.

All bold characters represent vectors or matrices. E [·] is the expected value of the bracketed expression.

The truth wind is equal to the predicted wind plus the error, or $\mathbf{w} = \mathbf{w}_o + \boldsymbol{\delta}\mathbf{w}$.
The covariance matrix is equal to the expected value of the square of the error matrix, or $\mathbf{C} = E[\boldsymbol{\delta}\mathbf{w} \cdot \boldsymbol{\delta}\mathbf{w}^T]$.

Step 1. Build the covariance matrix **C**, where $\mathbf{C}_{ij} = \rho_{ij} \cdot \sigma_i \cdot \sigma_j$

ρ_{ij} is the correlation between the errors at two altitudes (see Equation 2.2).

σ is the standard deviation for each component (see Table 2.3).

Step 2. Let $\boldsymbol{\delta}\mathbf{w} = \mathbf{S} \cdot \mathbf{v}$, where **v** is a vector of Gaussian random variables with zero mean and unity variance, so $E[\mathbf{v} \cdot \mathbf{v}^T] = \mathbf{I}$.

Step 3. Now $\mathbf{C} = E[\boldsymbol{\delta}\mathbf{w} \cdot \boldsymbol{\delta}\mathbf{w}^T] = E[\mathbf{S} \cdot \mathbf{v} \cdot \mathbf{v}^T \cdot \mathbf{S}^T] = \mathbf{S} \cdot \mathbf{S}^T$.

Step 4. Given **C**, solve for **S** from $\mathbf{C} = \mathbf{S} \cdot \mathbf{S}^T$.

Step 5. Generate the error vector from $\boldsymbol{\delta}\mathbf{w} = \mathbf{S} \cdot \mathbf{v}$.

Step 6. Generate the truth wind from $\mathbf{w} = \mathbf{w}_o + \boldsymbol{\delta}\mathbf{w}$.

Follow Steps 1-6 for both the North wind vectors and the East wind vectors.

2.5.2 Wind Profile Generation

It is also possible to generate wind profiles without any specific measurement data available. In order to generate the profile, the general wind statistics have to be known. The winds in the North and East direction were found to be zero mean and Gaussian from the balloon and radar data. Figure 2.15, shown below, displays the standard deviation of the winds as a function of altitude.

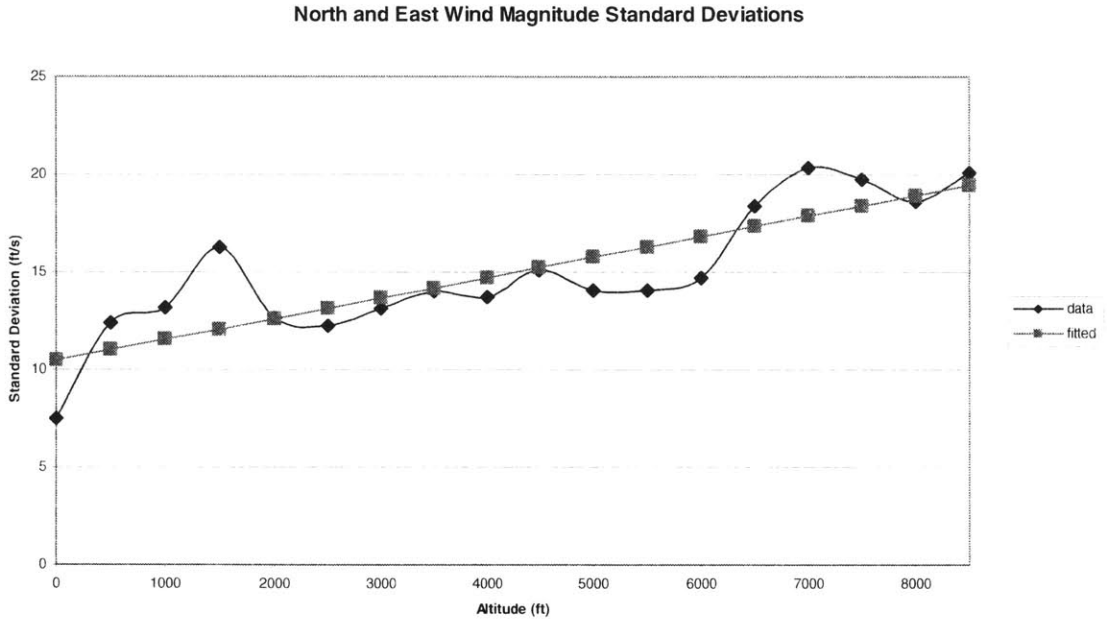

Figure 2.15. North and East Wind Magnitude Standard Deviations

Although the data in Figure 2.15 shows some non-linear behavior, there is a slight upward trend, implying that wind speeds increase with altitude. The fitted line shown has a slope of 1/950 s^{-1} and a y-intercept of 10.5 ft/s. Standard deviation is not enough to characterize the wind profile; the correlations between the winds at different altitudes are also required. Figure 16, shown below, displays the correlations between the wind velocities as a function of altitude difference.

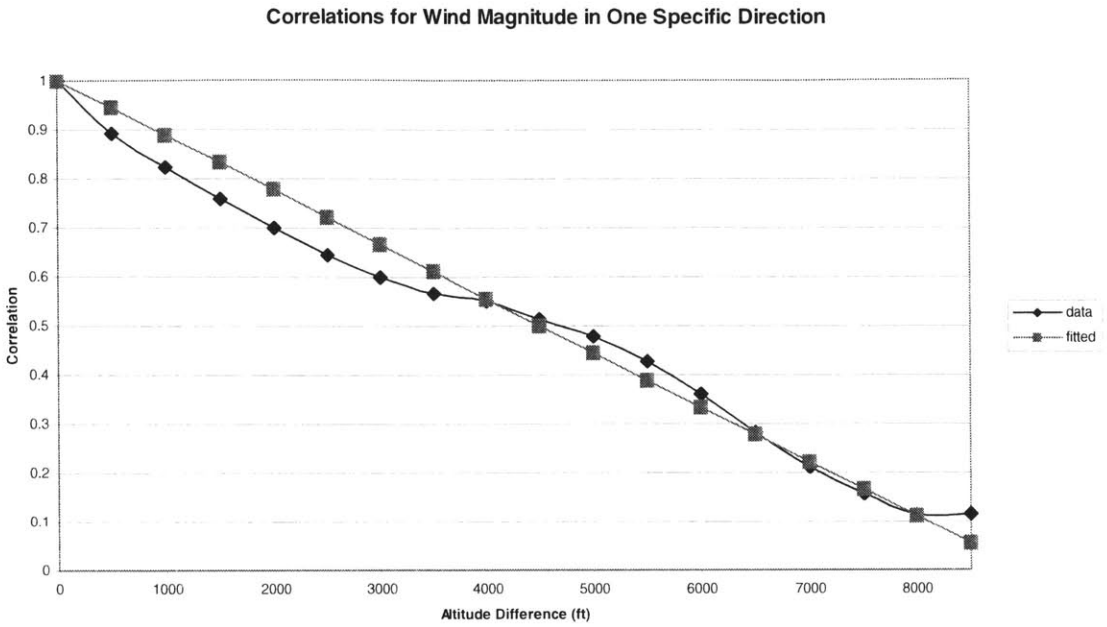

Figure 2.16. Correlations for Wind Magnitude in One Specific Direction

Unlike the correlations for errors at different altitudes, the correlations for the wind velocities are not exponential. The correlation curve in Figure 2.16 appears to follow a linear relation with respect to altitude difference, with a slope of 1/9000 ft^{-1}.

In order to generate a random profile with the given standard deviations and correlations, the same procedure is followed as in the North and East error method of truth wind generation. The only difference is that in this case, $\mathbf{w_o}$ is equal to zero.

The concepts of generating both predicted and truth winds are shown graphically in Figure 2.17. A random predicted wind was generated and plotted, along with the 3-sigma upper and lower limits for the wind error. Fifty truth winds were then generated and plotted on the graph. It can be seen that the fifty different truth wind profiles fall inside the 3-sigma error limits.

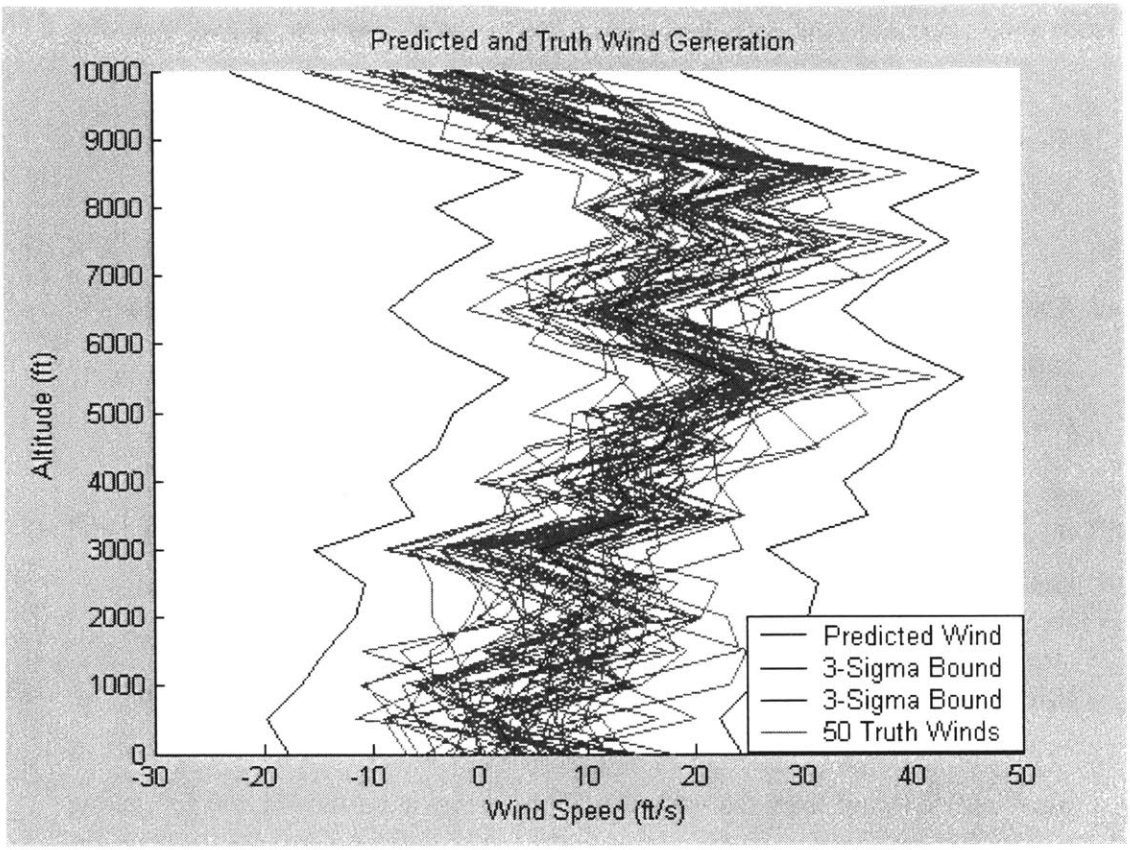

Figure 2.17. Predicted and Truth Wind Generation

2.6 Onboard Sampling

Guided airdrop systems can make use of insitu wind sampling as a way to decrease the errors that arise from a priori wind predictions. Onboard sampling can be used to update wind predictions from both general wind statistics and forecasting methods. An updated wind error profile is generated at each measurement and the guided parafoil will alter its position depending on the new wind error profile. The following steps outline the means of calculating correlated sample wind errors using the onboard sampling method.

All bold characters represent vectors or matrices. E [·] is the expected value of the bracketed expression.

The truth wind is equal to the predicted wind plus the error, or $\mathbf{w} = \mathbf{w}_o + \boldsymbol{\delta w}$.

Step 1. Measure the wind at the current altitude. Compare the measurement with the original prediction at that altitude to get the current wind error: $\boldsymbol{\delta w}_i$.

Step 2. The errors for the subsequent altitudes will be derived from the error at the current altitude with the formula: $\boldsymbol{\delta w}_{i+1} = \boldsymbol{\alpha}_{i,i+1} \cdot \boldsymbol{\delta w}_i + \mathbf{e}_{i+1}$, where $\mathbf{e}_{i+1}$ is a Gaussian random variable with zero mean and variance $\boldsymbol{\sigma}_{ei+1}^2$.

Step 3. $\boldsymbol{\alpha}_{i,i+1}$ can be found from the covariance ($\boldsymbol{\mu}$) between the errors at altitudes i and i+1 and the variance of the error at altitude i as follows.

$$\boldsymbol{\mu}_{i,i+1} = E[\boldsymbol{\delta w}_{i+1} \cdot \boldsymbol{\delta w}_i] = E[(\boldsymbol{\alpha}_{i,i+1} \cdot \boldsymbol{\delta w}_i + \mathbf{e}_{i+1}) \cdot \boldsymbol{\delta w}_i] = \boldsymbol{\alpha}_{i,i+1} \cdot E[\boldsymbol{\delta w}_i^2] = \boldsymbol{\alpha}_{i,i+1} \cdot \boldsymbol{\sigma}_i^2.$$

Step 4. $\boldsymbol{\sigma}_{ei+1}^2$ can be found from the variances of the errors at altitudes i and i+1, along with $\boldsymbol{\alpha}_{i,i+1}$ as follows.

$$\boldsymbol{\sigma}_{i+1}^2 = E[\boldsymbol{\delta w}_{i+1}^2] = E[(\boldsymbol{\alpha}_{i,i+1} \cdot \boldsymbol{\delta w}_i + \mathbf{e}_{i+1})^2] = \boldsymbol{\alpha}_{i,i+1}^2 \cdot E[\boldsymbol{\delta w}_i^2] + E[\mathbf{e}_{i+1}^2] = \boldsymbol{\alpha}_{i,i+1}^2 \cdot \boldsymbol{\sigma}_i^2 + \boldsymbol{\sigma}_{ei+1}^2.$$

Therefore $\boldsymbol{\sigma}_{ei+1}^2 = \boldsymbol{\sigma}_{i+1}^2 - \boldsymbol{\alpha}_{i,i+1}^2 \cdot \boldsymbol{\sigma}_i^2$.

Step 5. Generate $\boldsymbol{\delta w}_{i+1}$ from $\boldsymbol{\delta w}_{i+1} = \boldsymbol{\alpha}_{i,i+1} \cdot \boldsymbol{\delta w}_i + \mathbf{e}_{i+1}$ where $\mathbf{e}_{i+1}$ is randomly generated.

Step 6. Repeat Steps 2-6 for all desired altitudes to the ground altitude.

A more detailed explanation of this algorithm is provided in Chapter 4. This method of producing wind errors is fairly accurate because it involves a known error. However, the more recursions there are down towards the ground, the more error there will be due to the repeated random number generation. This method also only takes into account the correlation of the wind error between two successive altitudes, whereas the North and

East error method of truth wind generation (section 2.5.1) accounts for the correlations between all the errors.

If onboard sampling is being used for looking ahead to the winds at lower altitudes, the same procedure for generating correlated sample wind errors is used. The only difference is the known wind error is at whatever altitude the measurements are coming from, rather than the altitude that the airdrop device is currently at.

2.7 Limitations of Results

As with many error analyses, there are limitations to the credibility of the findings and this study is no exception. First of all, the general wind statistics and the balloon prediction wind data files used in this study are specific to the Yuma Proving Grounds in Yuma, AZ. Therefore, the results shown here may not be representative of other locations with different terrains and weather patterns. Another limitation of the results shown here is the fact that there was limited data to work with. Although the 32 predicted and truth files provided lots of data points, more data is always helpful in determining statistical parameters.

There are other methods available for wind predicting, and those methods were not studied. The data used here was for two types of wind prediction methods, general statistics and balloon prediction, and was the only readily available data. The balloon prediction method used here is only good for a couple hours after the measurement update is performed (e.g., balloon data). The numerical prediction models used here, using finite-difference methods to integrate the equations of motion, are believed to be one of the best prediction methods available. However, this type of prediction method is not always readily available, and other prediction methods not studied here will provide alternate statistical parameters.

Another imperfection of this analysis is that the measurements and predictions do not cover the exact same three-dimensional coordinates. The balloon is released at a certain

location, and travels upward into the sky collecting data to make the prediction. The parachute and/or windpack that record the truth winds do not fall in the exact path as the balloon ascension. However, due to the close proximity (usually within a mile or two), the truth winds are considered worthy enough to be compared to the predicted winds.

Finally, no vertical components of wind were taken into account in this study. Vertical winds can have a noticeable effect on the airdrop accuracy as they alter the sinkrate throughout the flight path. The main reason this effect was disregarded is that there was not available data for vertical winds.

2.8 Conclusions

When analyzing the effects of wind prediction errors on airdrop accuracy, this study will utilize both the wind prediction methods of general statistics, as well as assimilating the AFWA prediction with the balloon measurements. Unfortunately, this was the only reliable data available for wind prediction methods. However, balloon prediction is a good representation of forecasted wind prediction. This method is the most typical and most widely used technique, and therefore the results will be more meaningful than methods that aren't used as often. The forecasting method is considered the midpoint of quality when comparing the wind prediction methods, with general statistics being the lowest quality and onboard sampling being the highest. Therefore, this method can be regarded as an average wind prediction technique.

For the balloon prediction method, the average wind error in the North and East directions was found to be approximately 7 ft/s, with little relation to altitude. The correlation factor for this type of wind error was found to be approximately 900. If other methods were available, the same procedure for analysis can be implemented, and the corresponding wind statistics can be used in airdrop accuracy studies.

Both the general wind statistics and the AFWA/balloon wind prediction methods will be used when analyzing the performance of both unguided and guided airdrop systems. Guided airdrop systems will also be analyzed with onboard sampling methods.

Chapter 3
Unguided Air Release Planning System Error Analysis

3.1 Introduction

When comparing the benefits of various airdrop systems, it is important to know what causes some systems to perform better than others. In other words, it is important to know what the sources of airdrop errors are, and to what extent these errors contribute to the landing location error. Different classes of airdrop systems have different dominant errors, and it is beneficial to know the driving errors for these systems. Consequently, the benefits of more complex systems and the requirements for particular airdrop missions can then be evaluated.

The next two chapters are allocated to two different types of airdrop systems: unguided air release planning systems, and guided airdrop systems. This chapter is focused on determining the driving error sources for the first of these two types of systems, unguided air release planning systems. Total expected landing location errors and error sensitivities will also be examined.

3.2 Simulation Software

For error analysis with unguided air release planning systems, a simulation was used that was developed by a team at Draper Laboratory working with the Army Natick Soldier

Center under the New World Vistas (NWV) program. The simulation used for this study was PADS, or Precision Aerial Delivery System. More specifically, a version of PADS, known as PAPS (Precision Airdrop Planning System) was utilized. This simulation is a result of an effort with Draper Lab, the Army Natick Soldier Center, and several Air Force organizations to improve airdrop delivery accuracy.

The PADS simulation handles three degree-of-freedom dynamics models, along with experimental look-up tables, of unguided, ballistic airdrop systems. All phases of airdrop flight are analyzed, including: extraction, stabilization, steady-state descent, and landing. PADS can handle a variety of different aircrafts, parachutes, and payloads, among other variable parameters. Also included in the software is the capability for Monte Carlo simulation, which is useful in error analysis.

The initial simulation inputs for this study were taken from an actual airdrop performed by the NWV team at the Yuma Proving Grounds in Yuma, Arizona. The data is taken from one of a series of test drops on November 18, 2002. Many of the initial conditions for this airdrop were arbitrarily chosen as the initial conditions for all the simulation runs. Some of these conditions include: parachute type (26 foot ring-slot chute), North-East release position, release velocity, and aircraft type (C-130). Different parachutes and aircrafts could change some of the results, but the general trends of the errors are expected to be the same.

3.3 Airdrop Scenarios

In order to determine the driving errors of the airdrops, it is helpful to understand the types of conditions under which the drops are being done. For this study, a set of drop scenarios were established that would replicate typical drop conditions. These scenarios were based on four criteria: wind prediction methods, wind conditions, release altitudes, and payload weights.

For unguided systems, two types of wind prediction methods will be implemented: general wind statistics and balloon-driven forecasting. These wind prediction methods were discussed in the previous chapter.

Three different wind condition classifications were selected: light, medium, and heavy winds. Wind intensity levels are used in this study to examine the effects of overall wind intensity on airdrop accuracy. Determining what constitutes light, medium, and heavy winds is very subjective. The methods used in this study are just one of the seemingly infinite ways to describe the relative wind intensity.

The truth wind profiles that were used in the wind analysis in the previous chapter (from radar and windpack measurements) were taken, and all the North and East wind magnitudes were sorted in ascending order. These were then divided into three groups: the lower third was to represent light winds, the middle third for medium winds, and the upper third for heavy winds. The winds were to be modeled by a Gaussian distribution with zero mean and a standard deviation of sigma. The largest value in each division was defined as the three-sigma value for its particular classification of wind at the ground level altitude. The fact that we set this sigma value to the ground level is because wind magnitude was shown to increase with altitude in the previous chapter, and thus the sigma value will increase with altitude when developing wind profiles. This led to the following definitions:

Table 3.1. Wind Condition Definitions

Wind Condition	**Sigma (Ground Level)**
Light	3.5 ft/s
Medium	7.5 ft/s
Heavy	17 ft/s

These sigma values are used to produce wind profiles by the methods shown in the previous chapter. For the scenarios that use general wind statistics as the wind prediction method, different wind conditions are not used since the intensity of the wind is not recognized in any way.

Release altitude represents another facet of the airdrop scenario. Rather than studying many release altitude scenarios, two common altitudes were chosen: 10,000 ft and 25,000 ft. These two altitudes represent a mid-altitude test case and a high altitude test case that pushes the boundary of current operations. The final facet of the airdrop scenario is the payload weight. Three common payload weights were chosen for this study: 500, 1,000, and 2,000 pounds. These payload weights span the viable loading capabilities of the parachute being studied.

Combining these four components of the airdrop scenario, there are a total of 24 different combinations for scenarios to test the range of current operational missions. All 24 of these scenarios are simulated to determine what the driving errors are for unguided air release planning systems.

3.4 Typical Error Values

Seven parameters were recognized as major sources of error for unguided airdrops: exit time, release altitude, release course (also known as 'release heading'), release position, release speed, sinkrate, and wind. From data taken from past airdrops using the C-130 aircraft, the NWV team was able to derive typical error distributions for six of these parameters. The final error distribution, wind speed error, was derived in the previous chapter. Six of these parameters were found to have a Gaussian distribution. The non-Gaussian parameter, sinkrate error, was determined to be uniformly distributed. Their values are shown below in Table 3.2. Note that the North/East wind speed error is only for balloon-driven forecasting.

Table 3.2. Typical C-130 Error Values

Error Component	**Error (One σ)**
Exit Time	1.4 sec
Release Altitude	130 ft
Release Course	2 deg
Release Position	280 ft
Release Speed	20 ft/s
Sinkrate	Uniform on [- 5%, 5%]
North/East Wind Speed	7 ft/s

There are other parameters that could affect the accuracy of an airdrop as well. However, they are considered less important. This includes factors such as parachute uniformity and the dynamic model parameters of the parachute. This could affect many parameters, including but not limited to: drag coefficients, damping coefficients, and moments of inertia. These types of errors are not readily accessible to change in the current PADS/PAPS software, and are thus grouped together and assumed to be part of the sinkrate error.

3.5 Landing Errors from Individual Component Errors

In order to determine what the driving sources of errors are, it is effective to simulate each component error separately in a simulation; then observe the drop accuracy effects that each of the errors produces. The seven major sources of error, displayed above, were individually tested in the simulation in the following manner.

1) The simulation was run with nominal conditions.

2) The simulation was then run with one component altered by plus or minus one standard deviation of error.

3) This process was repeated with 100 different wind profiles and the average errors were calculated, along with standard deviations of the average error where applicable.

4) Steps (1) through (3) were repeated for all 24 scenarios

5) Steps (1) through (4) were repeated for the seven chosen sources of error.

This data was then collected and analyzed to determine what components caused the largest amount of landing location error under each scenario. The choice of altering the error sources by one standard deviation of error was because it provides a baseline for each error source even though the sources have dissimilar units. This way the relative effects of each error source can be examined during a typical mission. The standard deviation represents an upper bound of approximately two-thirds of all possible error values. Therefore, it is effective in portraying the effects of slightly more than the expected error value. For the uniformly distributed error, sinkrate error, the upper and lower bounds of the distribution were used.

Four of the error sources were found to produce the same landing location error regardless of the wind profile under each scenario. These will be referred to as release condition errors, and they were: exit time, release course, release position, and release speed. The reason they are referred to as release condition errors is because all the effects of the initial error happen before the parachute reaches steady-state descent; either in the extraction mode or stabilization mode. The wind has no major affect on the magnitudes of these errors because of the relative speed and time of these phases. The four release condition errors will now be discussed individually, followed by the remaining three steady-state descent errors.

3.5.1 Exit Time

Exit time is considered a flight-track error since the error in exit time alters the expected position of the payload along the flight track. If the exact error in exit time is known, the approximate effect on the landing location can be calculated. The error will be equal to:

$$\text{Landing Error} = (\text{Exit Time Error}) * (\text{Release Speed}) \tag{3.1}$$

For the C-130 sample airdrop that was used in this study, release speed was equal to 293.7 ft/s. With the one-sigma error value for exit time equal to 1.4 seconds, this gave a landing error of 411 feet for all scenarios.

3.5.2 Release Course

Error in release course is considered a cross-track error since this error alters the payload in the direction approximately orthogonal to the flight track. If the exact error in release course is known, the approximate effect on the landing location can be calculated as well. In this situation, there is a throw distance that the parachute experiences up until stabilization. If the release course is not as expected, the error will be approximately equal to the throw distance multiplied by the release course error angle, as shown in Figure 3.1:

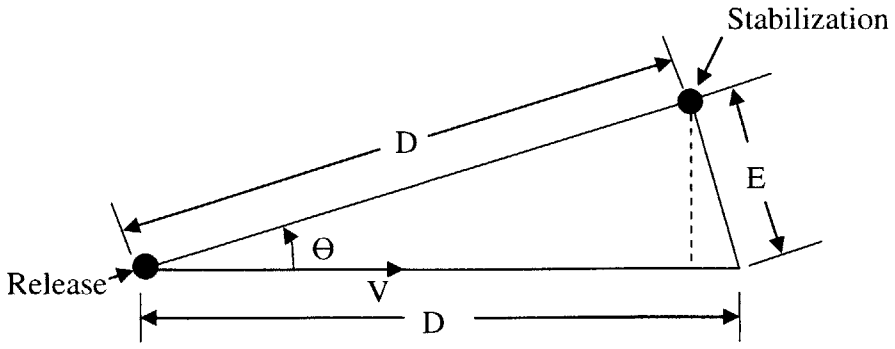

Figure 3.1. Release Course Error

In Figure 3.1, D represents the parachute's throw distance, Θ represents the release course error, and E represents overall location error caused by the release course error. Using trigonometry, one can derive the length of E as:

$$E = \sqrt{(D \cdot \sin\theta)^2 + (D \cdot (1 - \cos\theta))^2} \tag{3.2}$$

Using small angle approximations ($\sin(\Theta) \approx \Theta$, $\cos(\Theta) \approx 1$), Equation 3.2 simplifies to:

$$E = D \cdot \theta \tag{3.3}$$

Calculating the throw distance, D, is not so trivial. It is found by using a parameter known as the deceleration quotient (DQ). The DQ is a statistical parameter, and is the quotient found from dividing the forward throw distance in the stabilization phase by the release speed, with units of time [6]. Essentially, if the release speed is known, the throw distance in the stabilization phase can be calculated by multiplying the DQ with the release speed. The DQ is a function of payload weight and release altitude, and is found by inputting these two parameters into a lookup table developed by the U.S. military. The DQ is assumed constant for specific situations, but in reality it may differ slightly; thus all calculations using DQ are approximations. Using the DQ, the total throw distance can now be calculated:

$$D = V_{exit} \cdot (t_{exit} + DQ) \tag{3.4}$$

where V_{exit} is the release speed and t_{exit} is the exit time. The product $V_{exit} \cdot t_{exit}$ is referred to as the extraction distance, as it represents the ground-relative horizontal distance the payload moves while it is being moved out of the airplane. The product $V_{exit} \cdot DQ$ is referred to as the stabilization distance as it represents the ground-relative horizontal distance the payload moves while it is stabilizing itself in the air. Together, the sum of the extraction distance and the stabilization distance is the total throw distance. This is shown visually in Figure 3.2.

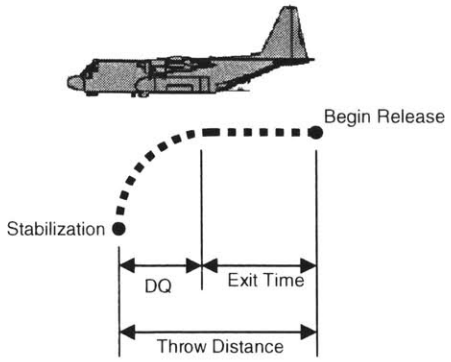

Figure 3.2. Parachute Throw Distance

For the C-130 sample airdrop that was used in this study, release speed was equal to 293.7 ft/s and exit time was equal to 5.1 seconds. The one-sigma error value for release course is equal to two degrees. All this gives a landing location error as a function of DQ, which in turn is a function of payload weight and altitude. Table 3.3 gives the landing location errors under each scenario for a one-sigma change in release course. The wind intensity and wind prediction methods are not taken into account since the wind is assumed to not affect the drop in the release condition phases; therefore there are six possible scenarios to be considered. The DQ value increases with both payload weight and release altitude. As a result, the error due to release course error increases with both payload weight and release altitude.

Table 3.3. Landing Location Error Due to a Two-Degree Release Course Error

Scenario		**Landing**
Payload (lb)	**Altitude (ft)**	**Error (ft)**
500	10000	82.0
500	25000	85.0
1000	10000	85.0
1000	25000	89.1
2000	10000	92.2
2000	25000	97.3

3.5.3 Release Position

Like the previous two error sources, the approximate effect that release position error has on landing location error can be calculated. In this case, whatever the release position error is, that is the same as the resulting landing location error. The airdrop is exactly the same, just shifted laterally in space. This is just an approximation, since it would not be the same value in reality. In the simulation used, the wind is assumed constant across every altitude. With different winds over an East-West grid, the landing location error would be different.

The one-sigma error value for release position is 280 feet. Thus, the landing location error due to release position error is 280 feet for all scenarios.

3.5.4 Release Speed

The final release condition error is release speed, and this is considered to be a flight-track error. Similar to the other three release condition errors, the approximate effect on landing location error can also be calculated, as shown:

$$E = \delta V_{exit} \cdot (t_{exit} + DQ) \tag{3.5}$$

where E represents landing location error, δV_{exit} represents the release speed error, t_{exit} represents the exit time, and DQ represents the deceleration quotient. Nominal exit time is equal to 5.1 seconds, and the one-sigma error value for release speed is equal to 20 ft/s. Again, wind is assumed not to be a factor in release condition errors, giving six possible scenarios for consideration when calculating the landing location error due to release speed, shown in Table 3.4. Similar to release course errors, landing errors due to release speed errors increase with DQ, and thus increase with payload weight and release altitude.

Table 3.4. Landing Location Error Due to a 20 ft/s Release Speed Error

Scenario		Landing
Payload (lb)	**Altitude (ft)**	**Error (ft)**
500	10000	160.0
500	25000	165.9
1000	10000	166.0
1000	25000	173.8
2000	10000	179.9
2000	25000	189.8

3.5.5 Release Altitude

The landing error due to error in release altitude is a steady-state descent error, meaning that the effects due to release altitude error propagate throughout the steady-state descent phase. Because of this effect, the landing error due to the release altitude error is not easily calculated.

Both the stabilization phase and the steady-state descent phase are affected by the release altitude error. However, the stabilization phase can be considered to be marginally affected. The change in altitude has an effect on the deceleration quotient, affecting the stabilization phase throw distance. The change in the deceleration quotient is small, but does have some effect on landing error. Since the parachute will stabilize at a different altitude, the wind will carry it on a slightly different path than a nominal drop would experience.

These effects are difficult to calculate, especially since they depend on wind conditions. Therefore, 100 simulations for each airdrop scenario were run to observe the effects of a one-sigma error in release altitude, and Table 3.5 summarizes the results below. Because wind is assumed to be known perfectly, different wind prediction methods were not used, giving 18 scenarios. Some expected trends were recognized while observing Table 3.5. As payload weight increases, the landing error decreases, due to the fact that the sinkrate

will be higher. Thus, there is less time for the wind to displace the parachute and payload. Also, as wind intensity increased, landing error also increased, as the faster winds were causing the parachute to be moved farther from the target compared to slower winds. Finally, landing error increased with release altitude, as there is more time of descent allowing the wind to move the parachute farther off target.

Table 3.5. Landing Location Error Due to a 130 ft. Release Altitude Error

Scenario			Landing Error (ft)	Standard Deviation (ft)
Payload (lb)	Altitude (ft)	Wind Intensity		
500	10000	Light	43.4	24.6
500	10000	Medium	64.5	36.8
500	10000	Heavy	96.7	54.0
500	25000	Light	90.7	46.7
500	25000	Medium	92.4	54.5
500	25000	Heavy	120.7	56.0
1000	10000	Light	35.8	20.1
1000	10000	Medium	41.3	19.0
1000	10000	Heavy	64.3	34.0
1000	25000	Light	55.8	25.6
1000	25000	Medium	74.9	33.7
1000	25000	Heavy	78.0	40.1
2000	10000	Light	23.0	12.7
2000	10000	Medium	32.6	16.8
2000	10000	Heavy	49.2	26.6
2000	25000	Light	40.9	24.2
2000	25000	Medium	47.0	18.5
2000	25000	Heavy	53.5	30.2

3.5.6 Sinkrate

Like release altitude error, landing error due to sinkrate error is difficult to analytically calculate. There are many parameters that affect sinkrate, including payload weight, air density, drag coefficient, and parachute surface area. Many of these will have simultaneous effects on the stabilization phase throw distance. Once the parachute has entered the steady-state descent phase, the change in sinkrate will cause a different

trajectory through the wind profile on its way down. Since these effects are not easily calculated to produce a landing location error, the same procedure was used as the release altitude error to observe the effects on landing error due to sinkrate error.

100 simulations were run for each scenario, and the results are summarized below in Table 3.6. As with release altitude error, there are 18 scenarios considered as different wind prediction methods are not analyzed. Sinkrate is uniformly distributed; therefore using a one-sigma error is not as valuable as for Gaussian errors. For that reason, an error of 5% was used to observe error effects. The observed effects on landing error are that landing error increases with release altitude and wind intensity and decreases with payload weight. These properties are due to the same reasons as discussed above with the release altitude error effects.

Table 3.6. Landing Location Error Due to a 5% Sinkrate Error

Scenario			Landing Error (ft)	Standard Deviation (ft)
Payload (lb)	**Altitude (ft)**	**Wind Intensity**		
500	10000	Light	81.2	47.4
500	10000	Medium	138.3	77.8
500	10000	Heavy	235.5	138.3
500	25000	Light	325.8	205.8
500	25000	Medium	361.7	203.6
500	25000	Heavy	551.7	274.9
1000	10000	Light	73.3	44.8
1000	10000	Medium	111.5	52.5
1000	10000	Heavy	163.5	88.5
1000	25000	Light	220.1	89.4
1000	25000	Medium	265.7	112.6
1000	25000	Heavy	355.4	178.1
2000	10000	Light	66.3	27.0
2000	10000	Medium	92.3	45.4
2000	10000	Heavy	121.9	60.8
2000	25000	Light	161.9	82.1
2000	25000	Medium	181.6	95.1
2000	25000	Heavy	261.5	143.1

3.5.7 Wind

The final component of error analyzed was wind knowledge. While the effects of the previous six components were tested by altering one standard deviation, that idea is difficult to implement with wind since there are so many values that have to be altered in the wind profile. For both general wind statistics and balloon forecasting, the methods outlined in the previous chapter were used to generate wind error profiles.

The landing errors due to wind knowledge error were also calculated using a Monte Carlo simulation. For each of the 24 scenarios, 50 simulations were run to collect statistical performance. The results are shown below in Table 3.7. There are 18 different scenarios for the balloon forecasting method, and only 6 different scenarios for the general statistics wind prediction method. This is due to the fact that when using the general statistics as a wind predictor, the intensity of the wind is not recognized in any way. Therefore, the only scenario parameters changed in the general wind statistics case are payload weight and release altitude.

The most recognizable trend in Table 3.7 is the large differences in error between the different wind prediction methods. Using general wind statistics as a wind prediction method gives significantly more error than using the balloon forecasting method. For 10,000 foot drops, the general statistics gives an error of about 250% of the error from balloon forecasting. For 25,000 foot drops, this error jumps up to 400%-600% of the error from balloon forecasting.

As with release altitude error and sinkrate error, landing error increases with release altitude, and decreases with payload weight. For the general wind statistics prediction method, error increases with wind intensity, but wind intensity was found to have no noticeable effect on the balloon forecasting prediction method. This happens because wind knowledge using balloon forecasting was shown to not be correlated with wind intensity, as shown in the previous chapter. Therefore, the same magnitudes of wind knowledge errors are implemented when altering light, medium, and heavy winds; thus producing similar errors for the same payload weight and release altitude values.

Table 3.7. Landing Location Error Due to Wind Knowledge Error

Scenario				Landing Error (ft)	Standard Deviation (ft)
Wind Prediction	**Payload (lb)**	**Altitude (ft)**	**Wind Intensity**		
General	500	10000	--	1996.6	1081.0
General	500	25000	--	6423.9	3226.3
General	1000	10000	--	1585.4	887.0
General	1000	25000	--	5137.3	2240.2
General	2000	10000	--	1058.5	697.9
General	2000	25000	--	3752.3	1769.6
Balloon	500	10000	Light	825.7	493.2
Balloon	500	10000	Medium	835.3	461.3
Balloon	500	10000	Heavy	852.7	501.5
Balloon	500	25000	Light	1520.7	769.7
Balloon	500	25000	Medium	1394.2	734.9
Balloon	500	25000	Heavy	1384.7	850.1
Balloon	1000	10000	Light	590.7	350.0
Balloon	1000	10000	Medium	568.0	328.3
Balloon	1000	10000	Heavy	604.2	356.9
Balloon	1000	25000	Light	1005.4	490.1
Balloon	1000	25000	Medium	1024.0	560.2
Balloon	1000	25000	Heavy	997.8	621.8
Balloon	2000	10000	Light	392.4	207.8
Balloon	2000	10000	Medium	429.4	205.9
Balloon	2000	10000	Heavy	443.1	224.1
Balloon	2000	25000	Light	685.7	329.8
Balloon	2000	25000	Medium	656.0	347.9
Balloon	2000	25000	Heavy	642.2	333.6

3.6 Dominant Errors

The preceding section outlined how each error source contributes to the landing location error under each scenario. It is also important to compare all of the error sources to each other for each scenario. This helps us to understand what the driving sources of error are. Once the main driving sources are known, efforts can be focused on reducing those errors. Using the data shown in the preceding section, the errors were compared to each other and listed in descending order under each scenario. These comparisons are shown below in Table 3.8, with the following abbreviations:

A – Release Altitude
C – Release Course
E – Exit Time
P – Release Position
Si – Sinkrate
Sp – Release Speed
W – Wind

Table 3.8. Error Source Comparisons

Scenario			Error Sources in Descending Order
Payload (lb)	**Altitude (ft)**	**Wind Intensity**	
500	10000	Light	W-E-P-Sp-C-Si-A
500	10000	Medium	W-E-P-Sp-Si-C-A
500	10000	Heavy	W-E-P-Si-Sp-A-C
500	25000	Light	W-E-Si-P-Sp-A-C
500	25000	Medium	W-E-Si-P-Sp-A-C
500	25000	Heavy	W-E-Si-P-Sp-A-C
1000	10000	Light	W-E-P-Sp-C-Si-A
1000	10000	Medium	W-E-P-Sp-Si-C-A
1000	10000	Heavy	W-E-P-Sp-Si-C-A
1000	25000	Light	W-E-P-Si-Sp-C-A
1000	25000	Medium	W-E-P-Si-Sp-C-A
1000	25000	Heavy	W-E-Si-P-Sp-C-A
2000	10000	Light	W-E-P-Sp-C-Si-A
2000	10000	Medium	W-E-P-Sp-Si-C-A
2000	10000	Heavy	W-E-P-Sp-Si-C-A
2000	25000	Light	W-E-P-Sp-Si-C-A
2000	25000	Medium	W-E-P-Sp-Si-C-A
2000	25000	Heavy	W-E-P-Si-Sp-C-A

Table 3.8 displays the error sources, in descending order, for each scenario. It can easily be seen that landing error due to wind estimation error is the major source of error for all of the scenarios. This is the case regardless of which wind prediction method is being utilized, and that is why only 18 scenarios are shown in Table 3.8, rather than 24. As previously shown, landing error due to wind estimation error increases with release altitude and decreases with payload weight. It can be inferred from that that while wind error is a dominant source of error for most low-altitude, heavy-payload airdrops, it is

even more of a dominant source of error for high-altitude and light-payload airdrops. By the same rationale, using general wind statistics rather than balloon forecasting will make wind even more of a dominant error as well. While different wind measurement systems can be shown to have higher or lower error standard deviations, it is still recognizable that wind estimation error is a major contributor to landing location error.

Exit time is also shown to have a significant impact on landing accuracy, as it is the second-most dominant error source in 17 out of 18 scenarios. Landing error due to exit time error is dependent on the aircraft's release speed. These comparisons are done for the C-130 aircraft, with a release speed of 293.7 ft/s. Although different aircrafts and different release speeds can be shown to have greater or smaller impacts on landing location error due to different release speeds, exit time should still be considered a major contributor of landing location error.

Three sources of error; release position, release speed, and sinkrate, make up the three moderate sources of error. They occur in different orders under different scenarios as shown in Table 3.8. They are not as dominant as wind error and sinkrate error, but are still considered to be relatively important when analyzing landing error. These three errors can be found to have different distributions for different aircrafts, avionics systems, and parachutes.

Errors in release course and release altitude represent the two smallest of the seven sources of error. Like many of the other sources of error, these two errors can also be found to have different distributions for different aircrafts, avionics systems, and parachutes, among other things. For example, landing error due to release course error will be smaller with a slower release speed. And depending on the type of altitude measurement system, the errors can be distributed differently for different altitudes.

Figures 3.3 and 3.4 show some specific results from the study. It can be deduced from the figures that the more time the parachute is in the air, the greater the landing error will be

due to wind estimation error, as the parachute in Figure 3.3 is in the air just over four times as long as the parachute in Figure 3.4.

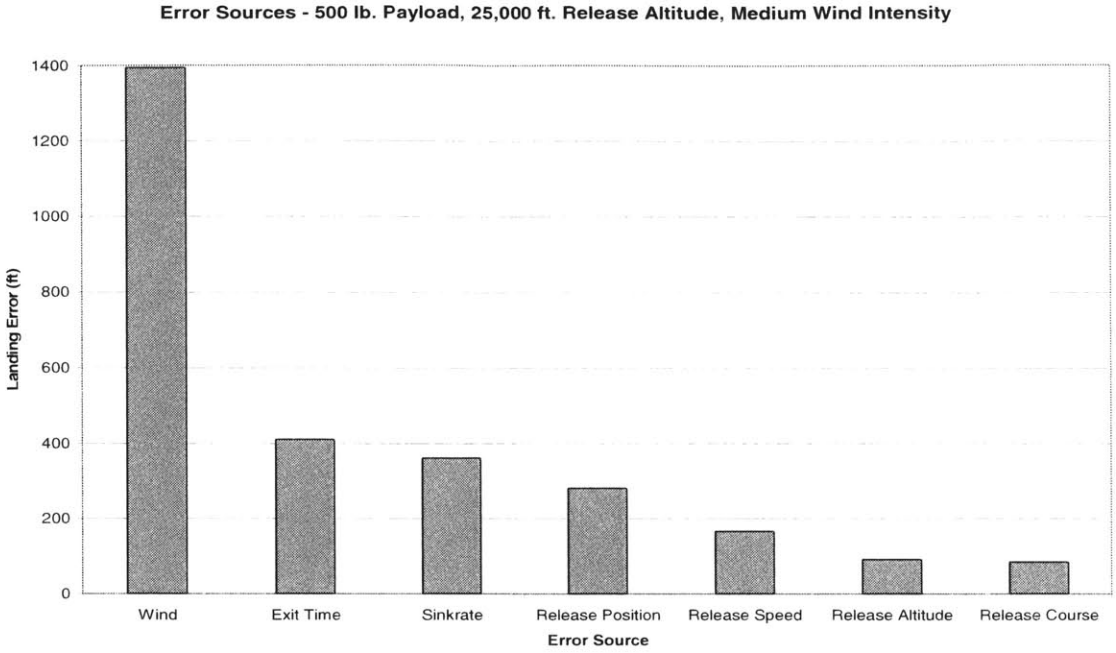

Figure 3.3. Error Sources – 500 lb. Payload, 25,000 ft. Altitude, Medium Wind Intensity

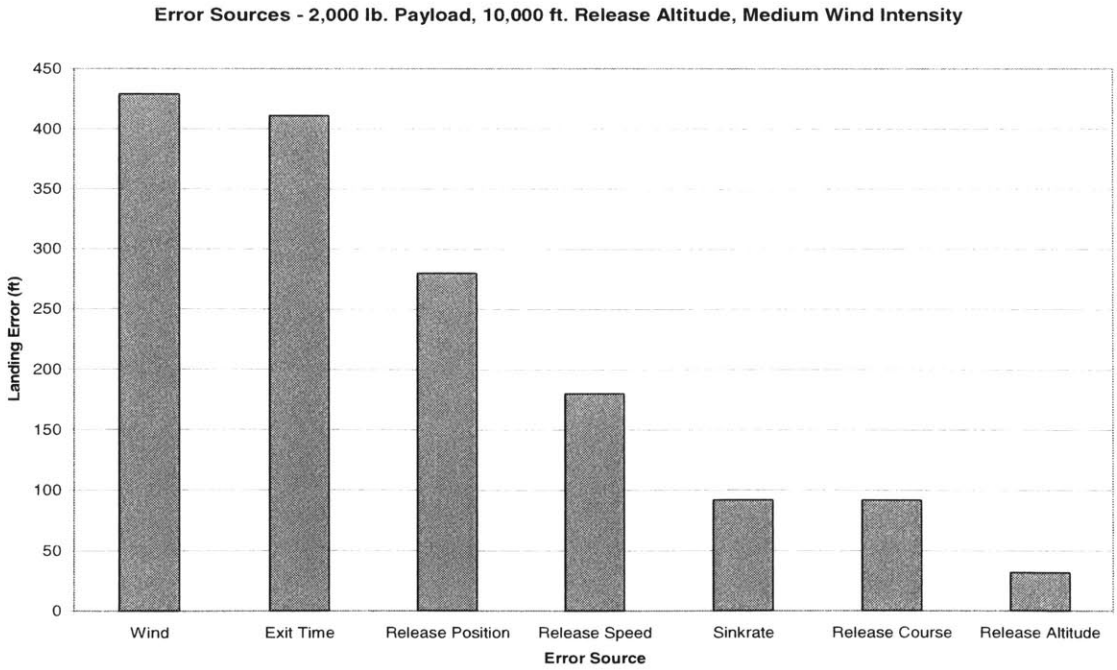

Figure 3.4. Error Sources - 2,000 lb. Payload, 10,000 ft. Altitude, Medium Wind Intensity

3.7 Total Landing Errors

As the general trends in component errors are identified, it is also useful to analyze the airdrops' landing location errors as a whole. For each scenario, 200-run Monte Carlo simulations were executed using the specified error distributions and wind error generating method. The averages and standard deviations of the landing location errors were then calculated, and are displayed below in Table 3.9.

Table 3.9. Simulated Landing Errors for 24 Chosen Scenarios

Scenario				Average Landing Error (ft)	Standard Deviation (ft)
Wind Prediction	**Payload (lb)**	**Altitude (ft)**	**Wind Intensity**		
General	500	10000	--	2132	1168
General	500	25000	--	7501	4206
General	1000	10000	--	1523	835
General	1000	25000	--	5338	2990
General	2000	10000	--	1079	592
General	2000	25000	--	3800	2126
Balloon	500	10000	Light	1067	560
Balloon	500	10000	Medium	1093	518
Balloon	500	10000	Heavy	1070	518
Balloon	500	25000	Light	1581	865
Balloon	500	25000	Medium	1574	867
Balloon	500	25000	Heavy	1587	779
Balloon	1000	10000	Light	957	388
Balloon	1000	10000	Medium	907	414
Balloon	1000	10000	Heavy	965	415
Balloon	1000	25000	Light	1162	558
Balloon	1000	25000	Medium	1194	635
Balloon	1000	25000	Heavy	1216	620
Balloon	2000	10000	Light	838	311
Balloon	2000	10000	Medium	837	297
Balloon	2000	10000	Heavy	836	319
Balloon	2000	25000	Light	944	428
Balloon	2000	25000	Medium	968	471
Balloon	2000	25000	Heavy	1044	469

Unlike some of the component errors, it is extremely difficult to calculate the total landing location errors exactly due to all the errors combined. One would not only need to calculate the landing location errors due to each component error, but also the directions of the landing location error components. They would then be added up vectorially. Because of this vectorial summation, adding each component error up will be larger than the actual total landing error. In some cases, the error may even be close to zero despite large component errors. Because these circumstances present difficult calculations, simulation was required.

There are some interesting trends to observe in Table 3.9. The obvious trend is that general wind statistics give much larger errors than scenarios that use the balloon forecasting. This situation proved true in the wind error section, and thus carried over into the landing location error. Another noticeable trend is the fact that landing location error seems to be completely uncorrelated with wind intensity for the balloon forecasting methods. It was shown before that landing location errors due to release altitude errors and sinkrate errors increase with heavier winds. However, when combined with all of the other errors, this heavy wind effect does not factor into the landing location error according to the PADS simulation. Nevertheless, landing location error is seen to increase with release altitude and decrease with payload weight. These were trends that were noticed earlier with the component errors.

The simulation shows the 10,000 foot airdrops to err approximately 800 to 1100 feet on average for the balloon forecasting wind prediction approach. This is comparable to actual airdrops performed by the NWV team at the Yuma Proving Grounds in November, 2002 and January, 2003. 15 successful drops were recorded during these months from 10,000 feet, with a variety of payload weights ranging from 1,090 to 2,235 pounds. The average landing location error was found to be 723 feet with a standard deviation of 532 feet. For these cases, the simulation appears to give slightly larger error values, but due to the limited number of test drops (15), more drops would be required to make a fair comparison.

3.8 Sensitivities and Error Reduction

The accepted method of reducing airdrop errors is to make efforts to reduce individual component errors. In an effort to reduce landing location errors, it is important to understand the sensitivities of landing location errors due to changes in component errors. In an effort to calculate the sensitivities, a similar approach was taken for each component as in the 'Landing Errors from Individual Component Errors' section. Each component's standard deviation of error was reduced by 50%, and the new landing location errors were observed and compared to the original landing location errors.

Three error source components were assumed to have a directly proportional relationship between the component error and the resulting landing location error. These error sources were release condition errors; and were exit time, release position, and release speed. Consequently, reducing these error sources by 50% provided a 50% reduction in the corresponding landing location error. Reducing the other release condition error, release course, by 50% does not provide a 50% reduction in the corresponding landing location error. This results from the non-linear trigonometric equation relating release course error to landing location error. Simulation showed that reducing release course error by 50% reduced the landing location error by about 25%.

The three steady-state descent errors do not have an explicit equation that shows a proportional relationship between the component error and their corresponding landing location errors. Intuition says that the three steady-state descent errors should be proportional to their corresponding landing location errors, and that is exactly what the simulations demonstrated. The standard deviation of error for release altitude and wind were reduced by 50%, and the outer limit of the sinkrate error's uniform distribution was shrunk by 50% to +/- 2.5%. These changes were implemented in the simulation, and produced corresponding landing location errors that were approximately 50% less than the previous errors under all scenarios.

Aside from release course errors, a 50% reduction in the individual component errors provides a 50% reduction in the resulting landing location errors. This information is beneficial in determining what error components should be focused on to reduce overall landing location error; i.e. to improve airdrop performance. Because all of the errors seem to have similar effects when reduced, it would be more advantageous to concentrate on the larger sources of error when attempting to reduce landing location error.

The fastest and easiest way to reduce error during an airdrop would be to add more weight to the payload. In every situation, the heavier the payload was, the less the error. Therefore, adding weight to the payload is a quick method to reduce landing error.

Wind and exit time errors were shown to be the most dominant sources of error. Implementing wind measurement systems that provide wind errors with standard deviations less than 7 ft/s would significantly reduce error. As would executing improved airdrop release procedures to reduce exit time error.

Improving the other errors would help overall landing error as well. Although this would not improve performance as significantly as improving wind and exit time errors by the same amount, improvements can still prove to be meaningful. As technology improves, measurement systems for release altitude, release course, release position, and release speed will reduce current errors for these error sources. Developing enhanced methods to better model the dynamics of the parachute and payload can help to reduce sinkrate error.

3.9 Conclusions

This chapter outlined the major sources of error for unguided airdrop planner systems. Seven sources of error were analyzed with the PADS simulation under 24 different scenarios. Wind measurement error and exit time error were found to be the most dominant sources of landing location error for all scenarios of airdrops. The other five sources of error were found to have a noticeable affect on landing location as well.

Using component error distributions derived by the NWV team, Monte Carlo simulations were run for each scenario to determine the average landing location error. Results for the simulated 10,000 foot airdrops showed comparable, although slightly greater, landing errors than actual test drops showed.

A simplified sensitivity analysis showed that reducing component errors by 50% reduced the corresponding landing location errors by 50% as well for six out of seven error sources. This reveals that efforts to reduce error should be concentrated on the larger sources of error, as they have more comparative landing location error improvement than the smaller sources of error.

Chapter 4
Guided System Error Analysis

4.1 Introduction

The previous chapter dealt with common errors that arise during airdrops from unguided air release planning systems. Errors that arise during airdrops due to the guidance and control of guided airdrop systems will now be examined. This will be beneficial when analyzing the benefits of adding a guidance system to airdrops, which will be presented in the next chapter.

This chapter will begin by describing the software used for simulation of guided airdrop systems. The type of parafoil used in the software will be briefly explained, as well as the general flight algorithm that the simulation executes. This will be followed by a description of the onboard wind measurement algorithms that were used in simulation, and then the types of different airdrop scenarios utilized. Total expected errors for these different scenarios will be displayed and analyzed. Recommendations for future research will be presented toward the end of the chapter.

4.2 Simulation Software

For error analysis with guided airdrop systems, a simulation was used that was cultivated by a team at Draper Laboratory working with the Army to develop precision guidance capability for parachute airdrop systems. This simulation is known as PGAS, or Precision

Guided Airdrop System. The simulation utilizes representations of parachute dynamics, navigation sensors, expected environment, and onboard wind measurement systems.

The type of parafoil used in this simulation is known as the "Wedge 3," which was developed by the NASA Dryden Flight Research Center (DFRC) [4]. The parafoil has a surface area of 88 square feet. Although PGAS has the ability to handle various types and sizes of parafoils, only one kind will be used to analyze the performance of guided airdrop systems.

During the simulation run, there are four distinct flight modes that the parafoil executes en route to the target [2]. The first of these four flight modes is known as the 'Maneuver to Way Point Submode.' This mode is how the simulation begins, if far enough away from the target. The predicted wind model is continuously integrated from the ground up to the current position to determine the total displacement due to wind. This displacement is then subtracted from the target location to form an updated target in an air-relative frame. This provides for easier maneuverability through the wind during descent. The parafoil simply heads directly toward the wind-adjusted target during this flight mode.

When the parafoil becomes close to the target, it enters into the second flight mode, known as the 'Holding Pattern Submode.' This mode is a way for the parafoil to reduce its altitude and stay close to the target. This mode could also be referred to as 'Energy Management Submode,' as the parafoil is essentially getting rid of excess potential energy. The parafoil circles around the target in a helix-shaped pattern to bleed altitude before it heads into a landing approach. As with the first flight mode, the displacement due to wind is continuously accounted for during descent.

At a certain altitude, the parafoil will be low enough to begin maneuvering towards the target. This is when the parafoil will enter the third flight mode, known as the 'Maneuver to Final Approach Submode.' During this phase, the parafoil exits the holding pattern helix and sets itself up for the final approach.

The final flight mode is the 'Final Approach Submode.' The parafoil does not align its heading angle directly toward the target throughout the entire final approach, but rather approaches in a spiral manner. The need for the spiral is to simultaneously reduce the altitude and radial error to zero, converging onto the target. This flight mode concludes with the parafoil landing.

Depending on the release conditions of the parafoil, some of these flight modes may not be utilized. For example, if the parafoil is released directly above the target with little wind to adjust for, the holding pattern will start immediately, thus skipping the first flight mode. Another example is if the parafoil is released far away from the target, it may not have enough energy to reach the target. In this case, the holding pattern will never be utilized to bleed altitude, thus skipping the second flight mode.

4.3 Onboard Wind Measurement Algorithms

The guided airdrop system uses a predicted wind profile to adjust its current position in order to minimize energy spent maneuvering against the wind. Due to the high variability and randomness of wind, often times the truth wind will be different enough that the predicted wind profile does not provide much help. Use of onboard wind measurement systems attempt to eliminate this problem, as they provide updated wind information for the guidance system to utilize.

At the beginning of the airdrop, the airdrop system has a predicted wind profile in its memory. Starting with the first wind measurement during descent, the predicted wind profile will change. The algorithm used in this study first simulates the measurement of the current wind. It then calculates the current wind error between the predicted wind profile and the measurement. That error is then used to propagate similar errors for all altitudes below the current one, taking into account the correlation of errors between different altitudes, as well as random effects. These errors are then added to the old predicted wind profile in order to generate a new predicted wind profile. The parafoil will then use the new predicted wind profile to adjust its position.

The following description, Table 4.1, is the algorithm used in this study to represent how onboard sampling develops a new predicted wind profile. E [·] is the expected value of the bracketed expression.

Table 4.1. Onboard Sampling Algorithm

1.	Measure the wind at the current altitude.
2.	Calculate the wind error (δw) by subtracting the current predicted wind from the current wind measurement.
3.	In order to calculate the wind error at the desired altitude (position 'i+1') from the current altitude (position 'i'), assume the relationship between the two errors to be of the form: $$\delta w_{i+1} = \alpha_{i,i+1} \cdot \delta w_i + e_{i+1} \quad (4.1)$$ where $\alpha_{i,i+1}$ is related to the correlation of the errors between the two altitudes and e_{i+1} is related to the randomness of the error. The parameter 'e' is assumed to be Gaussian with zero mean and variance σ_e^2. To calculate the values of $\alpha_{i,i+1}$ and e_{i+1}, it is first necessary to write out expressions for the covariance between the two errors and also the variance of the desired error.
4.	Covariance: $\mu_{i,i+1} = E[\delta w_i \cdot \delta w_{i+1}] = E[\delta w_i \cdot (\alpha_{i,i+1} \cdot \delta w_i + e_{i+1})] =$ $\alpha_{i,i+1} \cdot E[\delta w_i^2] = \alpha_{i,i+1} \cdot \sigma_{wi}$
5.	Now $\mu_{i,i+1} = \rho_{i,i+1} \cdot \sigma_{wi} \cdot \sigma_{wi+1}$, where $\rho_{i,i+1}$ is the error correlation between the two altitudes. Equating the two formulas and solving for $\alpha_{i,i+1}$ gives $$\alpha_{i,i+1} = \rho_{i,i+1} \cdot (\sigma_{wi+1}/\sigma_{wi}) \quad (4.2)$$
6.	Variance: $\sigma_{wi+1}^2 = E[\delta w_{i+1}^2] = E[(\alpha_{i,i+1} \cdot \delta w_i + e_{i+1})^2] =$ $\alpha_{i,i+1}^2 \cdot E[\delta w_i^2] + E[e_{i+1}^2] = \alpha_{i,i+1}^2 \cdot \sigma_{wi}^2 + \sigma_{ei+1}^2$
7.	Since $\alpha_{i,i+1}$ is now known, the error variance can be found: $$\sigma_{ei+1}^2 = \sigma_{wi+1}^2 - \alpha_{i,i+1}^2 \cdot \sigma_{wi}^2 \quad (4.3)$$
8.	Using Equations 4.2 and 4.3, a random error can be generated. Thus, all the variables are known to solve Equation 4.1 for δw_{i+1}.
9.	Continue this recursive process for each altitude level used all the way to the ground level to develop an error profile.
10.	To develop the new predicted wind profile, add the newly developed error profile to the old predicted wind profile.
11.	Repeat steps 1-10 as the parafoil descends down to the ground.

Another application of the onboard sampling algorithm is to use it to represent 'look-ahead sampling.' Look-ahead sampling measures the wind at a future location, rather than the current location, to update the predicted wind profile. In theory, this is supposed to provide better accuracy than measuring the current wind since the system knows more about what is happening in the area that it is headed towards. Both onboard sampling and look-ahead sampling were analyzed in this study.

4.4 Airdrop Scenarios

For this study, a set of drop scenarios were established that would replicate typical drop scenarios. These scenarios were based on five criteria: release altitudes, payload weights, wind prediction methods, wind conditions, and onboard wind measurement systems. Three release altitudes were studied: 5,000, 10,000 and 15,000 feet. Also, three payload weights were considered: 100, 200, and 300 pounds. Using the 88 square foot parafoil, these weights gave similar weight loadings (pounds per square foot) as the unguided parachute in the previous chapter.

Three types of wind prediction methods were considered that spanned the range of wind knowledge capabilities. These types are: no wind knowledge, general statistics, and balloon-driven forecasting. In the cases where there was no wind knowledge, the airdrop system assumes there is no wind at all. During this situation, the target is not offset to account for displacement due to wind. The other two wind prediction methods, general statistics and balloon-driven forecasting, were discussed in detail in chapter two. For these two methods, the target location is constantly adjusted to account for the predicted future displacement due to wind.

Wind conditions, classified as light, medium, and heavy, were discussed in chapter three (see Table 3.1). For drops that used no wind knowledge or general statistics as a means to predict wind, there is no way to know how strong the wind is before the drop. Therefore, these separate wind conditions were only analyzed with balloon-driven forecasting airdrops.

The final facet of the airdrop scenario is the type of onboard wind measurement system being utilized. First, the airdrops were simulated using no type of onboard wind measurement system. Second, the airdrops were simulated using the basic onboard sampling, where the wind at the current altitude is measured. Third, the airdrops were simulated using look-ahead sampling, where wind is measured at a location below the current location. For simplicity, all look-ahead samples were measured at an arbitrarily-chosen distance of 1500 feet below the current altitude, which happens to represent an estimate of the capabilities of a relatively cheap LIDAR system.

4.5 Errors in Guided Airdrop Systems

There are many errors that occur during guided airdrops, and some of these errors can affect the landing accuracy. There are basically three general types of uncertainties that result in error for guided airdrop systems. These are: uncertainties in release conditions, sensor errors, and uncertainties in wind knowledge.

During an airdrop, the parachute is released in the air and it goes through a stabilization phase during which the chute opens and the system approaches a steady-state descent. Any errors that occur from uncertainties in release conditions basically just change the position in the air that the steady-state descent begins. The PGAS simulation used in this study does not include any release or stabilization effects, and essentially begins the simulation in the steady-state descent mode. Thus in order to simulate errors in release conditions using this software, the initial position conditions would be shifted by an amount corresponding to the errors in the release conditions. For guided systems, these errors are assumed to be small enough that the guidance system onboard will in essence cancel them out. Therefore, errors in release conditions were not analyzed in this study.

A guided airdrop system has a guidance system that could consist of several navigation sensors. These usually include the GPS (Global Positioning System), an INS (Inertial Navigation System), a barometric altimeter, a magnetic compass, and a ground-relative

altimeter. Each one of these sensors has errors in their measurements, which will affect the performance of the airdrop system. However, the purpose of this chapter is to determine how to improve guided airdrop performance through guidance and control. The navigation errors are essentially decoupled from the guidance and control errors, and they will not be analyzed in this study. If they were studied, the errors would be continuously added on by superposition throughout descent.

The last type of error is the uncertainty in wind knowledge. This plays a key role in guided airdrop systems, as the wind knowledge affects the guidance and control of the system. As the parachute is descending toward the ground, the airdrop system uses a predicted wind profile to adjust its current position in order to minimize energy spent maneuvering against the wind. Due to the high variability and randomness of wind, the error in the calculation of the displacement due to wind can be significantly large that the parafoil maneuvers way off course. Sometimes, this improper maneuvering causes the parafoil to position itself so far off course that the target can never be reached. This type of error is the only error examined for guided airdrop systems in this study.

4.6 Monte Carlo Description

For many of the scenarios defined for guided airdrop systems, Monte Carlo simulations were executed to determine the expected landing location errors of the scenarios. Each scenario generated a Monte Carlo analysis of 200 runs. Prior to the descent phase for each of these runs, a predicted and truth wind profile would be generated. The parafoil would calculate the displacement due to wind from the predicted wind profile, and that offset defines the initial release position. The parafoil then descends toward the ground, updating the target location due to wind throughout the flight. The drops that use an onboard wind measurement system continually update the wind knowledge the entire time. Upon landing, the distance away from the target is calculated. This process was repeated 200 times for each scenario.

Figure 4.1, shown below, displays a scatterplot of the landing locations that resulted from a 200-run Monte Carlo sequence. This scenario uses balloon forecasting as the wind prediction method, a 200 pound payload, a 5,000 foot release altitude, and medium wind intensity.

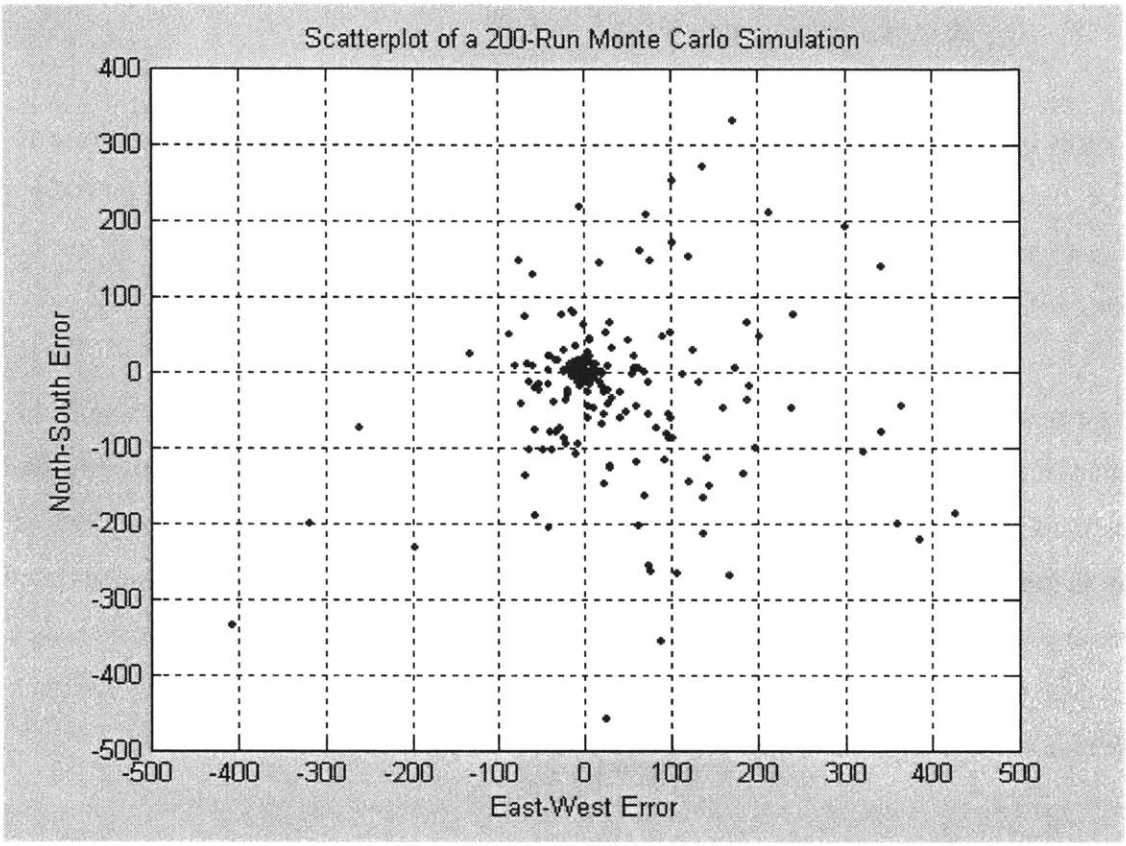

Figure 4.1. Scatterplot of Landing Errors (ft) for a 200-run Monte Carlo Sequence

For this particular scenario, this data gives an average landing error of 103.2 feet with a standard deviation of 120.5 feet. The median in this case is much smaller than the mean, as can be inferred by looking at the histogram and noticing the large concentration of data points close to zero. At 64.3 feet, the median is about 62% of the mean. Out of the 200 simulations in this Monte Carlo sequence, approximately 2/3 of the drops had an error that was less than the mean.

The mean is not equal to the median due to the non-Gaussian impact dispersion. This large discrepancy between the median and the mean is caused by several extremely large

errors. Although there is a 50% chance that the balloon forecasting will give you a performance of less than 64.3 feet of landing error under these circumstances, there is still a chance that the error can be upwards into the 500 foot range. This type of distribution is also representative of most of the other scenarios. There is generally a large concentration of smaller errors, and there are several extremely large errors that skew the average to be much greater than the median.

For most of the outlying data points, high winds or high wind prediction errors were to blame. If the winds are fast enough, the parafoil will have difficulty maneuvering through the air to where it wants to go. If the wind prediction errors are great, the parafoil will be biasing itself in the wrong direction in anticipation of the expected wind.

For purposes of comparing the performance of each scenario, both the mean and the median of the landing location errors will be used. The median is also sometimes referred to as the CEP, or circular error probable, because it represents the distance that 50% of your landing errors will fall within. The medians will be used since the means can oftentimes be misleading due to the outlying data points. However, using the mean makes it simpler when later comparing unguided and guided systems, as the unguided systems were also compared by their means (also referred to as their expected values).

4.7 Expected Landing Errors

For each unguided airdrop scenario in the previous chapter, 200-run Monte Carlo simulations were executed using the specified predicted and truth wind profile generating methods. The expected landing errors for the unguided airdrop systems under 90 different scenarios were then calculated. In this chapter, however, all 135 of the defined scenarios were not executed. The reason for this is that during some trial simulation runs, many trends were observed that showed the parafoil's accuracy behaving similarly under different scenarios, and thus demonstrating that there was no distinction between these different cases. Therefore, running Monte Carlo simulations for those similar situations

would be redundant. Several variables showed this redundancy, and it was concluded that those variables had no or negligible effect on the parafoil's landing accuracy.

The first variable that was found to have negligible effect on landing accuracy was release altitude. This is a different result than from the unguided study, where landing errors increased as release altitude increased. For the guided system, if the parafoil is dropped off high enough, the parafoil will enter a holding pattern as it bleeds altitude. Regardless of how high above that point the parafoil will drop, the parafoil will exit the holding pattern at a similar altitude, thus developing similar errors on its final approach to the target. Figure 4.2, shown below, displays an example of how release altitude does not have an effect on the landing error. For this case, the following were held constant: no wind knowledge, no onboard wind measurement systems, and a 200 pound payload.

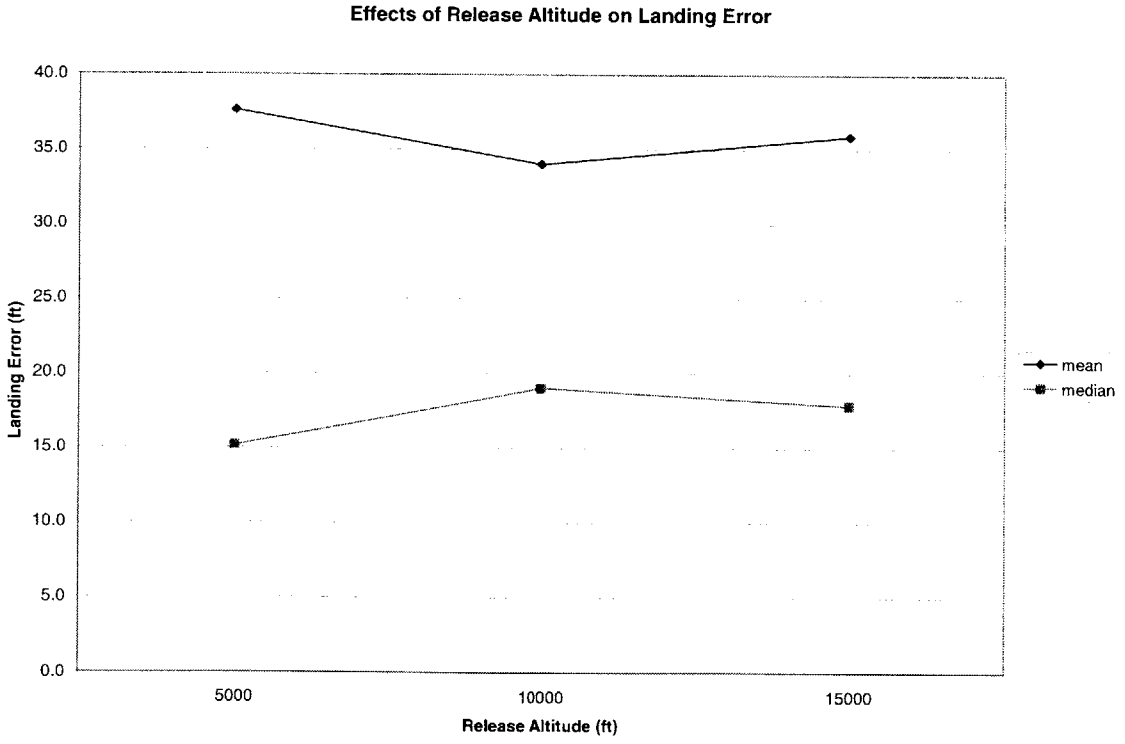

Figure 4.2. Effects of Release Altitude on Landing Error

Another variable that was found to have negligible effect on landing accuracy was payload weight. A heavier payload weight meant that the parafoil would be traveling at

faster speeds. These faster speeds showed no noticeable effects on landing accuracy, as the faster parafoils performed just as well as the slower parafoils. Figure 4.3, shown below, displays an example of how payload weight has negligible effect on landing error within reasonable loading conditions. For this case, the following were held constant: no wind knowledge, no onboard wind measurement systems, and a 5,000 foot release altitude.

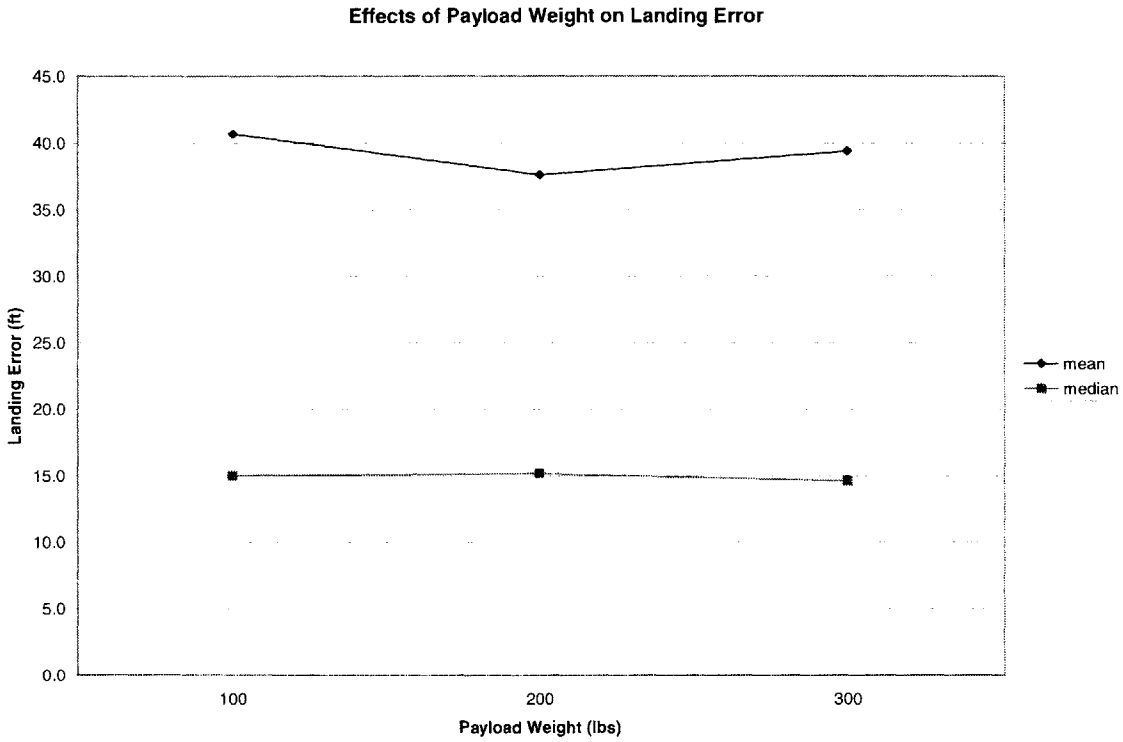

Figure 4.3. Effects of Payload Weight on Landing Error

The last variable that was found to have negligible effect on landing error was wind intensity. Wind intensity only played a factor when using balloon forecasting as a wind prediction method, as no other wind prediction methods studied can predict the current intensity of the wind. In Chapter 2, it was shown that wind prediction error is not correlated with wind intensity. Therefore, the same magnitude of wind errors are implemented when altering light, medium, and heavy winds; thus producing similar wind offset errors. Figure 4.4, shown below, displays an example of how wind intensity does not have an effect on landing error. For this case, the following were held constant:

balloon wind knowledge, no onboard wind measurement systems, a 200 pound payload, and a 5,000 foot release altitude.

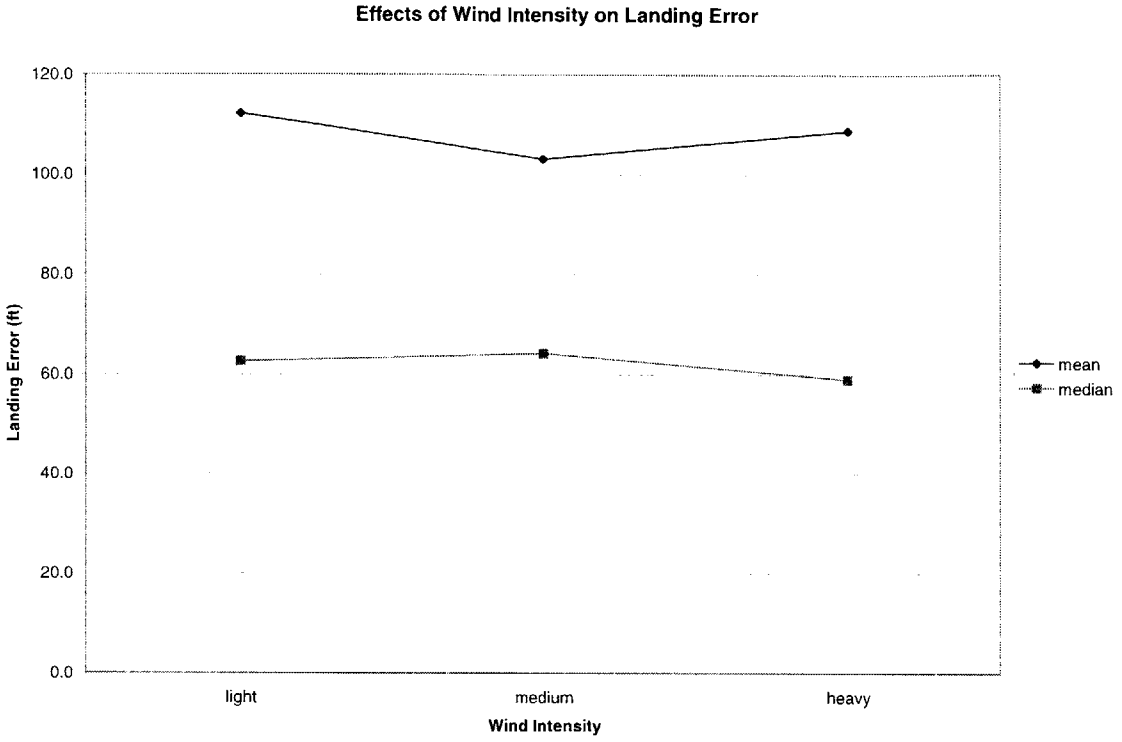

Figure 4.4. Effects of Wind Intensity on Landing Error

Payload weight, release altitude, and wind intensity were found to have negligible effects on landing accuracy for guided airdrop systems. The two factors that displayed differences in landing accuracy will now be analyzed. Those two factors are the type of wind knowledge used, and the type of onboard wind measurement system used. For consistency, the following variables were set during the rest of the guided airdrop study: 200 pound payload, 5,000 foot release altitude, and medium winds (balloon forecasting only). Figure 4.5, shown below, displays the landing errors that result from the three types of wind knowledge without using any onboard wind measurement systems.

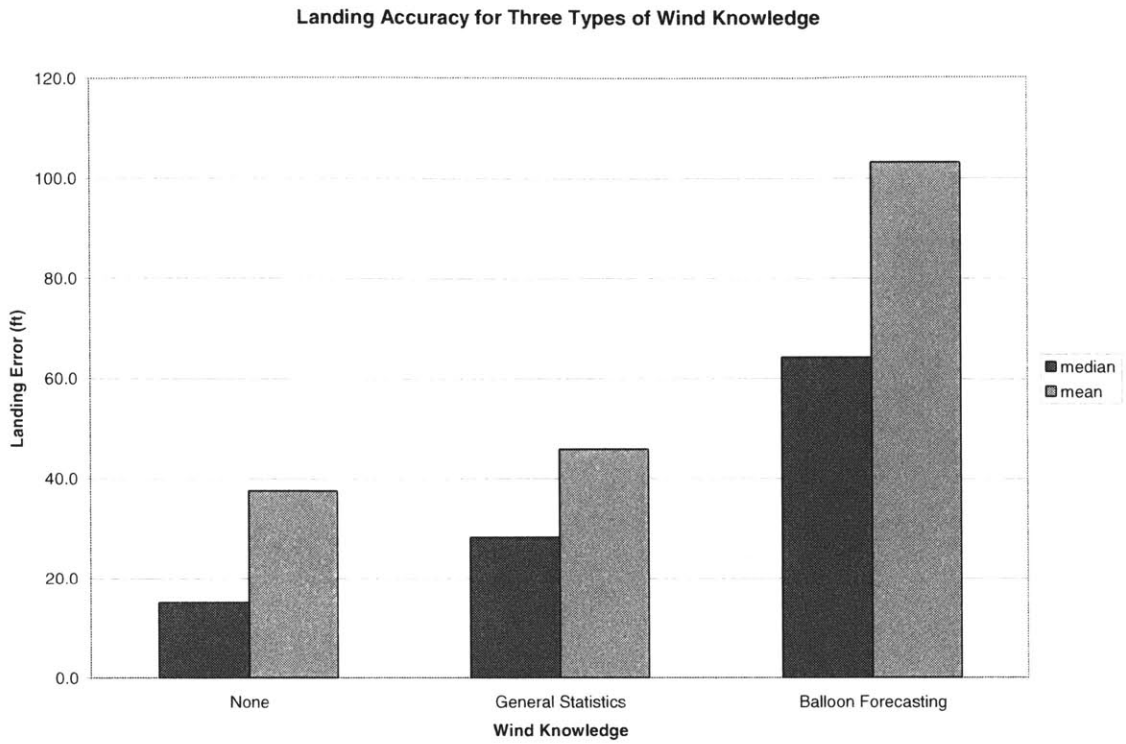

Figure 4.5. Landing Accuracy for Three Types of Wind Knowledge

Figure 4.5 shows that as your wind knowledge becomes better, your landing accuracy becomes worse. This type of behavior was unexpected, but the reason for this is explainable. The way the simulation is set up, if there is wind knowledge being used, the parafoil will calculate the horizontal distance that the wind will cause the parafoil to move as it descends toward the ground, and then offset the target according to this distance. These calculations are done with the predicted wind, which has a certain error to it with respect to the actual wind. In the simulation, the balloon forecasting wind prediction method has an error standard deviation of seven feet per second on the ground, while the general statistics wind prediction method has an error standard deviation of approximately four feet per second on the ground. The greater the wind prediction errors near the ground, the greater the parafoil will incorrectly offset its position.

Figure 4.5 also shows that not using any wind knowledge performs better than both of the wind knowledge situations. This is due to the fact that the parafoil is able to maneuver through the wind and stay on course relatively well throughout the drop. By not

attempting to offset the target, it doesn't incur any offsetting errors and remains close to the target. However, this logic breaks down if the winds are so heavy that the parafoil has difficulty maneuvering through them. This will be shown in the next two figures.

Figure 4.6, shown below, displays the trajectories of three simulated airdrops. The wind conditions are identical for each of the three drops, and are classified as medium-intensity winds. The payload was equal to 200 pounds and the release altitude was 5,000 feet. The solid line is the trajectory of the drop without using any wind knowledge. The parafoil was able to come close to the target in this situation. The two dashed lines are examples of drops using balloon forecasting. Because the offset target was generated with considerable error, the parafoil did not come as close to the target as before.

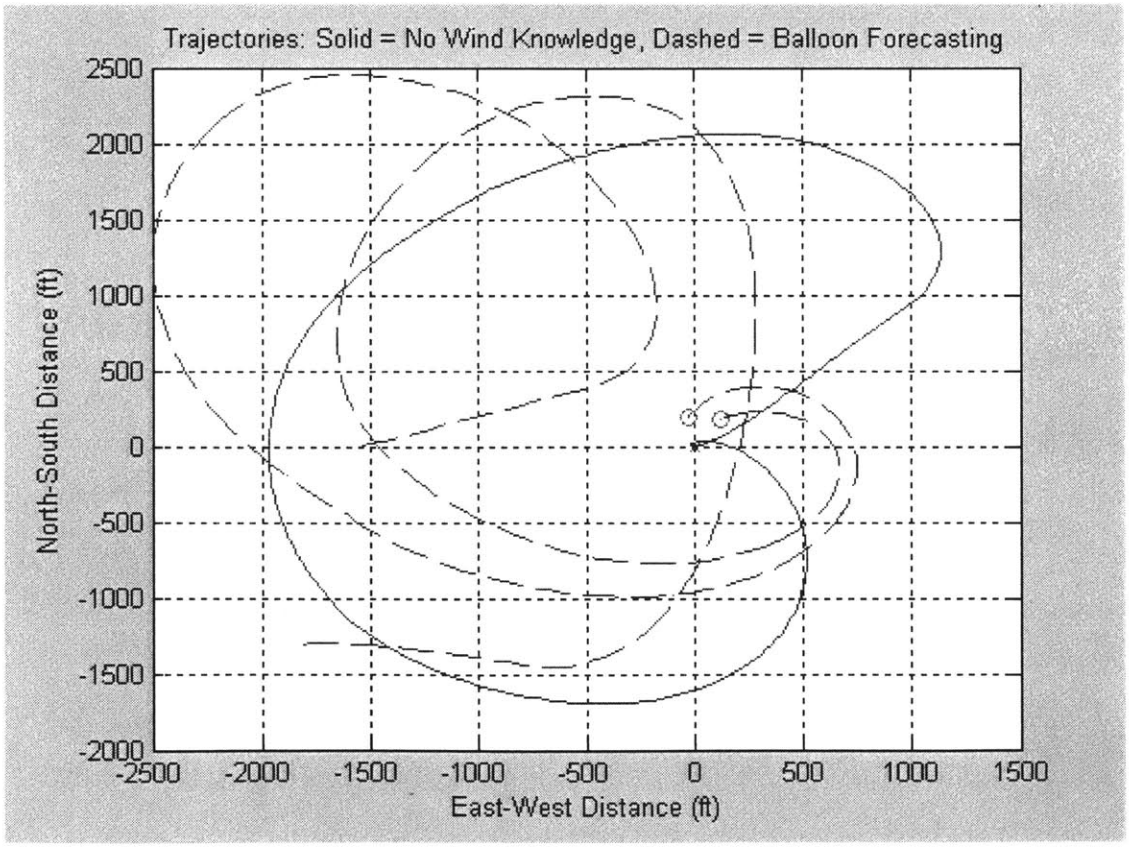

Figure 4.6. Trajectories under Medium-Intensity Winds

Figure 4.7, shown below, again displays the trajectories of three simulated airdrops. The wind conditions are also identical for each of these drops, but this time the wind conditions were very heavy. The same wind profile from the previous figure was used, and all the individual values were multiplied by a factor of four. The payload was also equal to 200 pounds and the release altitude was 5,000 feet. Under these circumstances, the drops that used balloon forecasting landed closer to the target than the drop that didn't use any wind knowledge. The balloon-forecasted drops performed similar to the balloon-forecasted drops under medium-intensity winds. However, the airdrop that didn't use any wind knowledge had difficulty maneuvering through the heavy wind; thus landing further away than before.

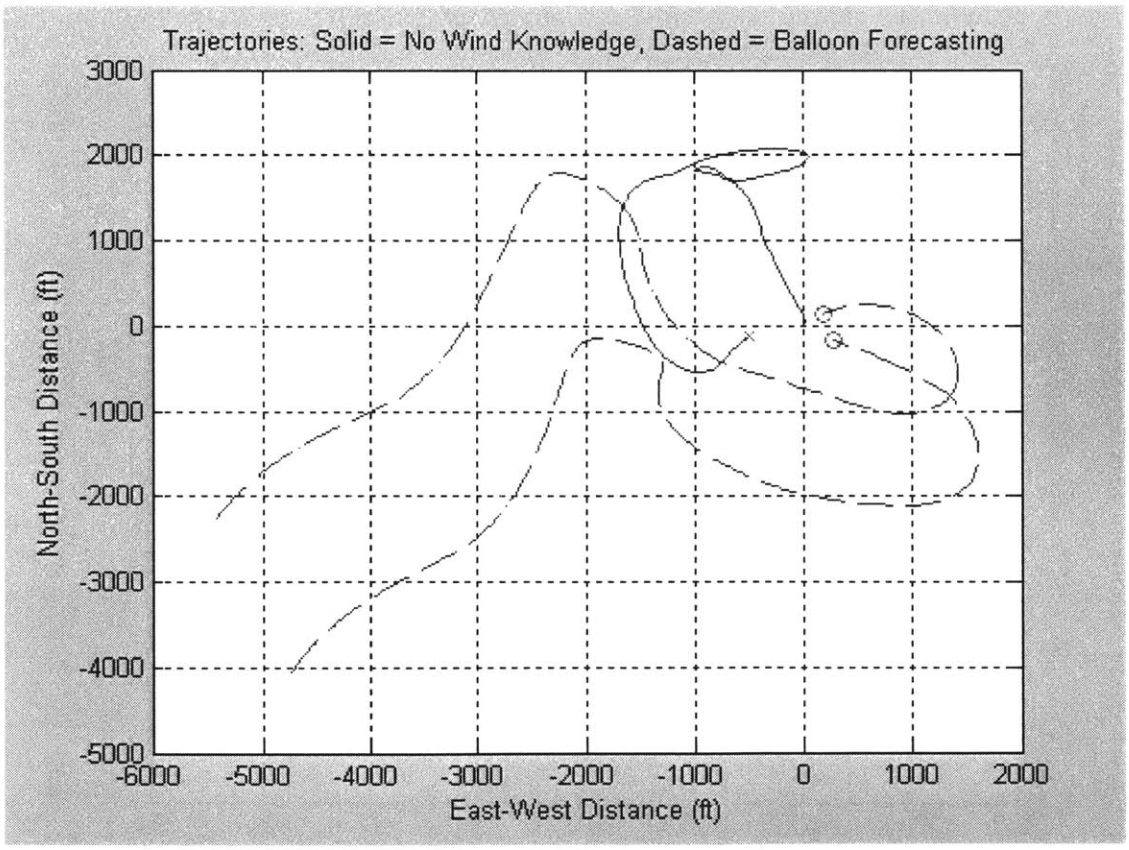

Figure 4.7. Trajectories under Heavy Winds

Figure 4.8, shown below, displays another example of landing errors as the wind intensity increases. A constant West wind was inputted into the simulation and the landing errors were calculated two cases: no wind knowledge and balloon forecasting.

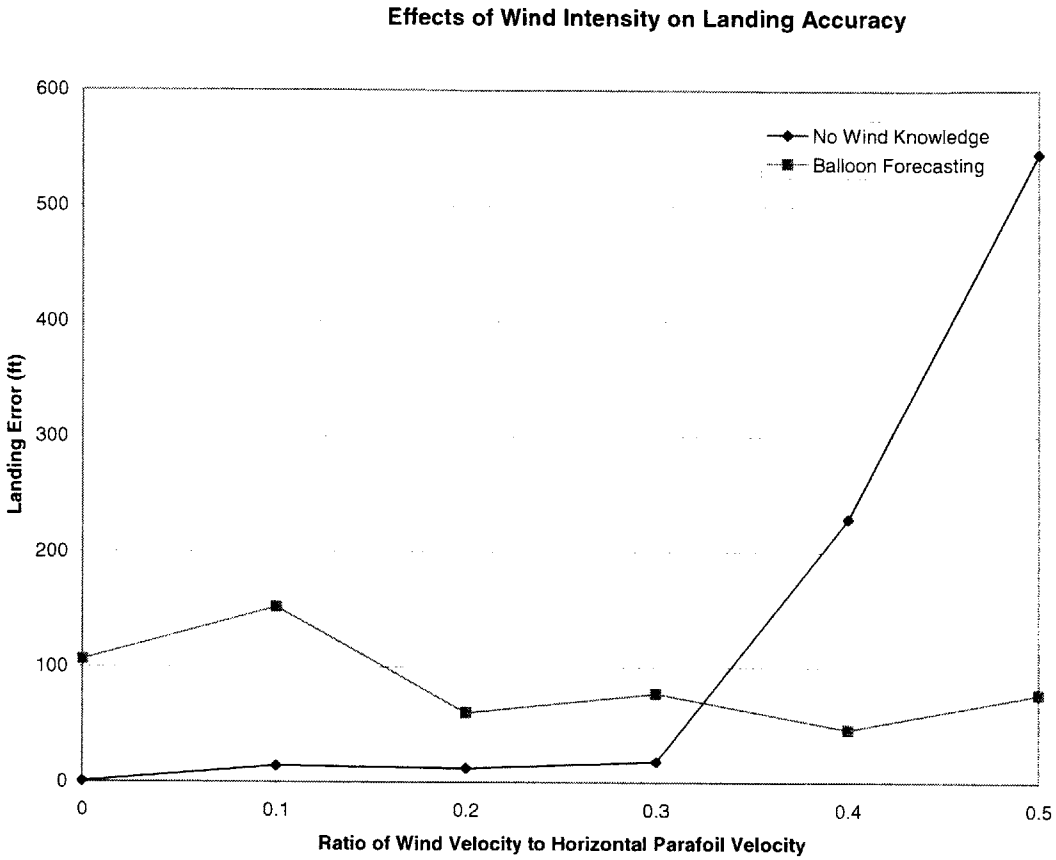

Figure 4.8. Effects of Wind Intensity on Landing Accuracy

For a 200 pound payload, the horizontal air-relative velocity is 41.2 feet per second. For a ratio of 0.1, that means that there was a constant West wind of 4.12 feet per second. Figure 4.8 demonstrates the superiority of not using any wind knowledge at low winds. It also demonstrates the fact that as wind speeds get higher, there comes a point where the parafoil can not maneuver as well as it wants to and errors start accumulating. Since wind intensity does not affect the error due to balloon forecasting, the errors continue to stay approximately the same regardless of wind speed.

Figure 4.8 is just one example using the ratio of wind velocity to horizontal parafoil velocity. A ratio of 0.4 is often encountered in flight, and the plot shows that when the ratio approaches this value, errors begin to accumulate when not using wind knowledge. However, this will not always be the case for a ratio of 0.4. The results used in this plot depend on many factors, such as where the parafoil is as it maneuvers toward the final approach. Setting the wind to a constant speed in a different direction will yield different numbers, although the general trend will remain the same.

The use of onboard wind measurement systems were also implemented in the simulations. In this study, when the measurement system measures the wind at the parafoil's current location, that is referred to as onboard sampling. When the measurement system measures the wind at a point below the parafoil's current location, that is referred to as look-ahead sampling. For this study, the simulated look-ahead distance was chosen to be 1500 feet. This was chosen since using a look-ahead distance of 1500 feet with no a priori wind knowledge closely resembled the performance of using perfect wind knowledge, as shown below in Figure 4.9. In Figure 4.9, all the look-ahead simulation runs used no a priori wind knowledge. All the simulation runs, including the perfect wind knowledge case, used a 200 pound payload and a 5,000 foot release altitude.

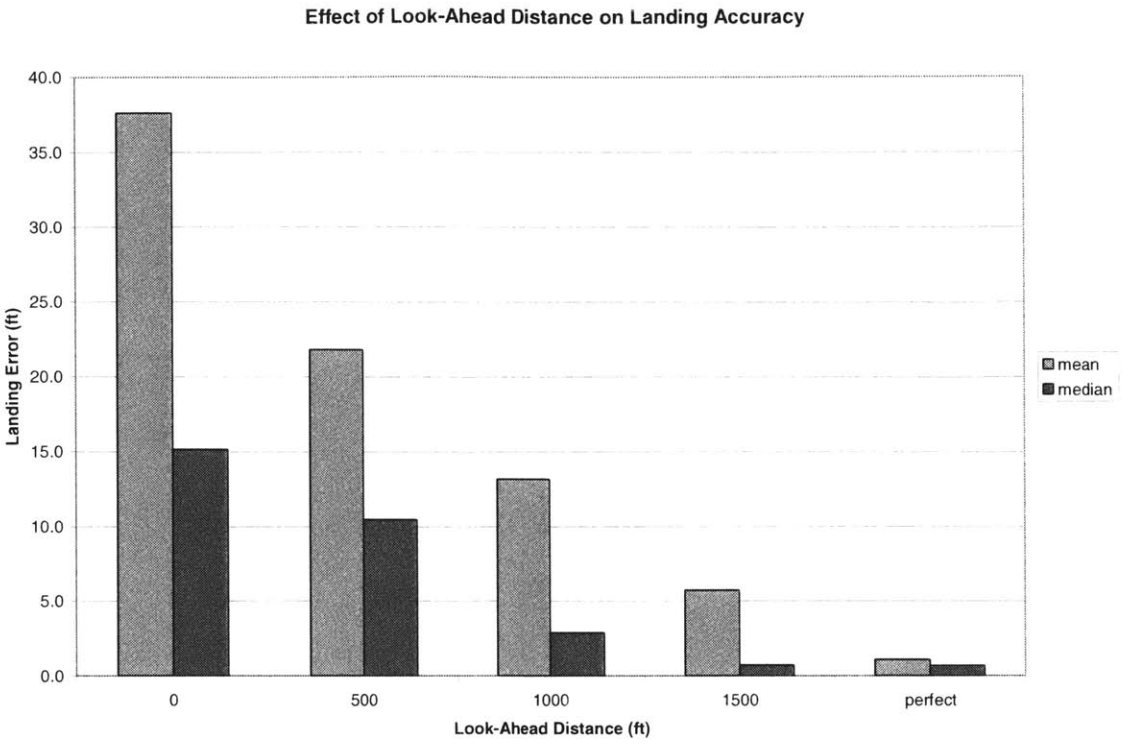

Figure 4.9. Effect of Look-Ahead Distance on Landing Accuracy

The two factors that define the scenario (wind knowledge and onboard wind measurement system) combine to make nine different scenarios. The expected landing error for these nine scenarios is shown below in Figure 4.10.

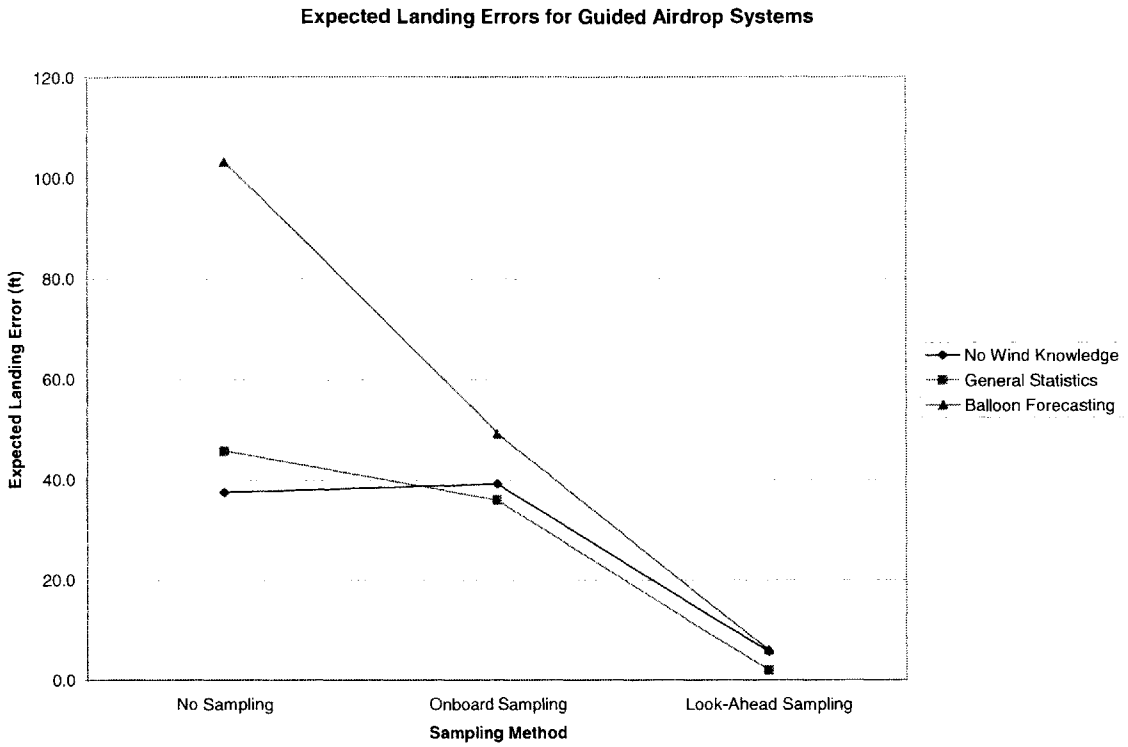

Figure 4.10. Expected Landing Errors for Guided Airdrop Systems

From Figure 4.10, it can be seen that using sampling results in similar landing accuracy regardless of what type of wind knowledge is available. Sampling the wind does prove beneficial towards landing accuracy when compared to no sampling, and the further ahead the sampling measures, the more accurate the airdrop will be. Figure 4.10 also shows that when using a guided system to perform an airdrop, in general, using no wind knowledge is just as good, if not better, than using some other type of wind knowledge. The exception, as previously discussed, is when the winds are relatively high compared to the parafoil's horizontal air-relative velocity.

Figure 4.11, shown below, illustrates the differences in the wind profiles between onboard sampling and look-ahead sampling. In this situation, the payload is released at an altitude of 2,000 feet with no wind knowledge. There is a constant East wind at 10 feet per second. Using onboard sampling, the wind at the current altitude is measured and the sampling algorithm develops a new prediction, as shown in the figure. Using look-ahead sampling, the wind is perfectly known down to an altitude of 500 feet. The parafoil is at a

typical altitude to begin its landing approach, and the wind knowledge developed from look-ahead sampling is far superior to the wind knowledge developed from onboard sampling. Thus, it is expected that the parafoil using look-ahead sampling will outperform the parafoil using onboard sampling.

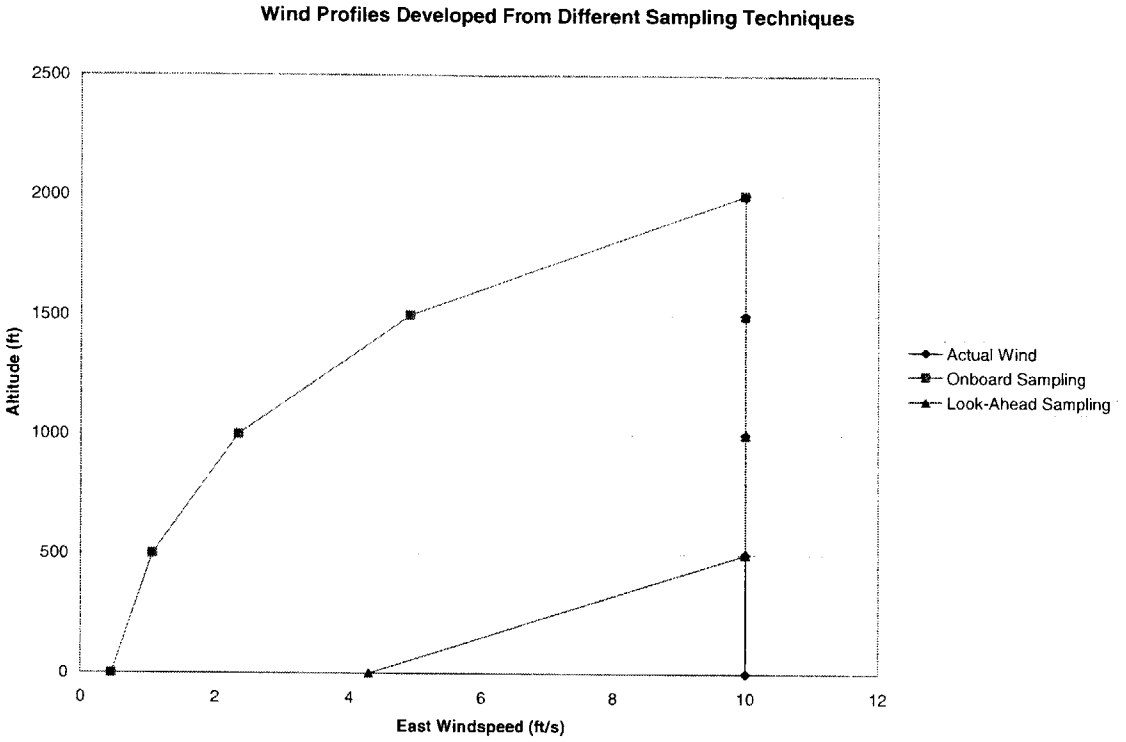

Figure 4.11. Wind Profiles Developed From Different Sampling Techniques

4.8 Limitations of Results

As with many error analyses, there are limitations to the credibility of the findings and this study is no exception. These limitations can open the door to other research endeavors as a continuation of this study. One limitation of this study is that only one guidance algorithm was used. The simulation used in this study, PGAS, has a certain guidance logic that the parafoil follows as it guides and controls itself to the target. There are other guidance algorithms used in parafoil simulations that might not exactly coincide with the results of this study.

Many guided parafoil systems attempt to land the parafoil while heading into the wind [2]. This reduces the forward ground speed of the parafoil in an attempt to reduce the impact on the ground. Heading into the wind also serves the purpose of reducing lateral errors caused by the wind. As the parafoil makes its final turn toward the target, it does not have much time to correct for errors that wind may cause. The PGAS simulation does not land in a straight path, but in a radial path that is continually updated as it approaches the target. Using a system that attempts to land into the wind could change the accuracy of the airdrop.

Another limitation of this study is that a relatively small parafoil was used in simulation. Larger parafoils could provide different results than what the smaller parafoils provide, especially since the larger parafoils generally have a slower yawing rate and faster airspeed. This will affect how quickly the parafoil can react to its environment. For example, if the wind suddenly pushes the parafoil off course, the smaller parafoils can turn back toward its course quicker than the larger parafoils can. Analyzing the handling abilities of different size parafoils would be beneficial to understanding the benefits of guided systems in general.

Finally, one other limitation in this study is that the wind models used here may be overly-conservative near the ground, where the landing accuracy performance is particularly sensitive. Wind is known to have a high-variability near the ground depending on the surrounding terrain, and this study doesn't take that into account. Implementing a wind model with higher variability near the ground could lead to different landing accuracies.

4.9 Conclusions

This chapter analyzed errors that arise during airdrops due to the guidance and control of guided airdrop systems for different airdrop scenarios. These scenarios were then compared to each other to determine what types of wind prediction knowledge and

onboard wind measurement systems displayed the best performances. Not using any wind knowledge proved to be an adequate method of using a guided system. Using wind knowledge, such as general statistics or balloon forecasting didn't show to be of much help as compared to not using any wind knowledge. The exception being when there are heavy winds.

Onboard wind measurement systems showed to be a good addition to guided airdrop systems. The further the look-ahead distance for the measurement, the more accurate the airdrop will be, as the system more closely resembles a perfect wind knowledge airdrop.

Chapter 5
Airdrop Planning Aid

5.1 Introduction

The past two chapters demonstrated the types of errors that are inherent in both unguided air release planning systems and guided airdrop systems. They also displayed the expected landing errors under different scenarios. In this chapter, the data will be taken and put in a form that is useful when planning an airdrop. The procedure outlined in this chapter is not a complete product, but can serve as a template for future airdrop planning aid design.

A major issue to keep in mind during this chapter is that these results are only completely valid for the particular systems analyzed in this study; those being the PADS and the PGAS systems. While some insights can be taken away from this chapter, the final numbers may be different with other systems.

5.2 Guidance Determinants

When performing an airdrop, the airdrop personnel need to know what steps should be taken to ensure a certain landing accuracy. The question being asked is: If I have to land this payload within a particular distance of the target, what do I need to do to my airdrop system in order to land within that distance? This question can also be reversed: With the

airdrop system that I have now, how big of an area do I need to ensure that the payload lands in that area?

The previous two chapters outlined the expected errors for both an unguided air release planning system and a guided airdrop system, respectively. This data will now be portrayed in a different format, in a manner that will be beneficial when planning an airdrop. The previous two chapters gave means and standard deviations of landing location errors for various scenarios. These values are important, but when planning an airdrop, it is more important to know what size of a clearing is needed to guarantee a safe landing. The parameter that will be used to describe this area will be known as the 'required landing area radius,' as the area will be defined as a circle.

When a Gaussian random variable is described with a mean and a standard deviation, a distance of two standard deviations from the mean encompasses approximately 95% of the distribution. This 95% value will be used to define the required landing area radius for all scenarios, and this radius is equal to the landing location error's mean value plus two standard deviations. Table 5.1, shown below, displays the required landing area radii for all the unguided airdrop scenarios.

Table 5.1. Required Landing Area Radii for an Unguided Air Release Planning System

Scenario		Mean Landing Error (ft)	Standard Deviation (ft)	Required Landing Area Radius (ft)
Payload (lb)	Altitude (ft)			
500	10000	1067	560	2187
500	25000	1581	865	3311
1000	10000	965	415	1795
1000	25000	1194	635	2464
2000	10000	836	319	1474
2000	25000	1044	469	1982

In Chapter 3, it was found that wind intensity did not have an effect on landing error for unguided air release planning systems, just wind estimation error. Therefore only six scenarios are being shown here rather than the previous 18 scenarios. The values shown in Table 5.1 all use balloon forecasting as the wind prediction method. General statistics

will not be discussed here as the errors were too large to be of practical use. Using general statistics as a means of predicting wind for unguided systems resulted in required landing area radii of between 3,500 and 13,000 feet.

Nine different scenarios were used in the guided airdrop studies. The corresponding required landing area radii for these nine scenarios are shown here in Table 5.2.

Table 5.2. Required Landing Area Radii for a Guided Airdrop System

Scenario		Mean Landing Error (ft)	Standard Deviation (ft)	Required Landing Area Radius (ft)
Wind Knowledge	Sampling Method			
None	None	37.6	44.4	126.3
None	Onboard Sampling	39.2	59.5	158.2
None	Look-Ahead Sampling	5.7	36.0	77.8
General Statistics	None	45.9	51.7	149.4
General Statistics	Onboard Sampling	36.0	56.5	149.1
General Statistics	Look-Ahead Sampling	2.0	31.1	64.2
Balloon Forecasting	None	103.2	120.5	344.2
Balloon Forecasting	Onboard Sampling	49.3	56.1	161.5
Balloon Forecasting	Look-Ahead Sampling	6.1	36.8	79.7

It is clear from Tables 5.1 and 5.2 that the guided airdrop system outperforms the unguided system. There is absolutely no overlap between the two. When determining what type of system will be useful for a particular airdrop, a good place to start is determining whether or not to use a guided system. For 95% confidence given the simulation model and data used in this thesis, if the landing area radius is 1400 feet or greater, an unguided air release planning system will be adequate. If the landing area radius is less than 1400 feet, it will be necessary to use a guided system, where the radii fall between 64 feet and 344 feet. Figure 5.1 visually displays the differences in landing areas between unguided and guided systems. The large circles represent required landing areas for unguided systems and have an approximate radius of 1600 feet. The small circles represent required landing areas for guided systems, and have an approximate radius of 200 feet. With guided systems, there are obviously more locations that are suitable for landing.

Figure 5.1. Landing Areas for Unguided and Guided Systems

5.3 Unguided Air Release Planning Aid

If the airdrop planner determines that an unguided parachute using balloon forecasting will be adequate enough for the drop, the next step in the planning process will be to determine either what release altitude to drop from or what is the required landing area radius given the release altitude.

Looking at Table 5.1, one can determine what combination of payload weight and release altitudes are necessary to land within a specified radius. The same trends are shown here as were discussed in Chapter 3: for unguided air release planning systems, landing accuracy increases with an increase in payload weight and a decrease in release altitude.

A script was developed using Matlab, named altcalc.m, that can be used as a tool to determine an adequate release altitude for unguided air release planning systems. The only options for release altitudes are the two that were simulated in this thesis, 10,000 ft. and 25,000 ft. Due to the limited number of data points acquired in this study, other release altitudes are not able to be interpolated using altcalc.m. Figure 5.2 displays the decision process for altcalc.m. Diamond shapes represent decisions and rectangles represent actions.

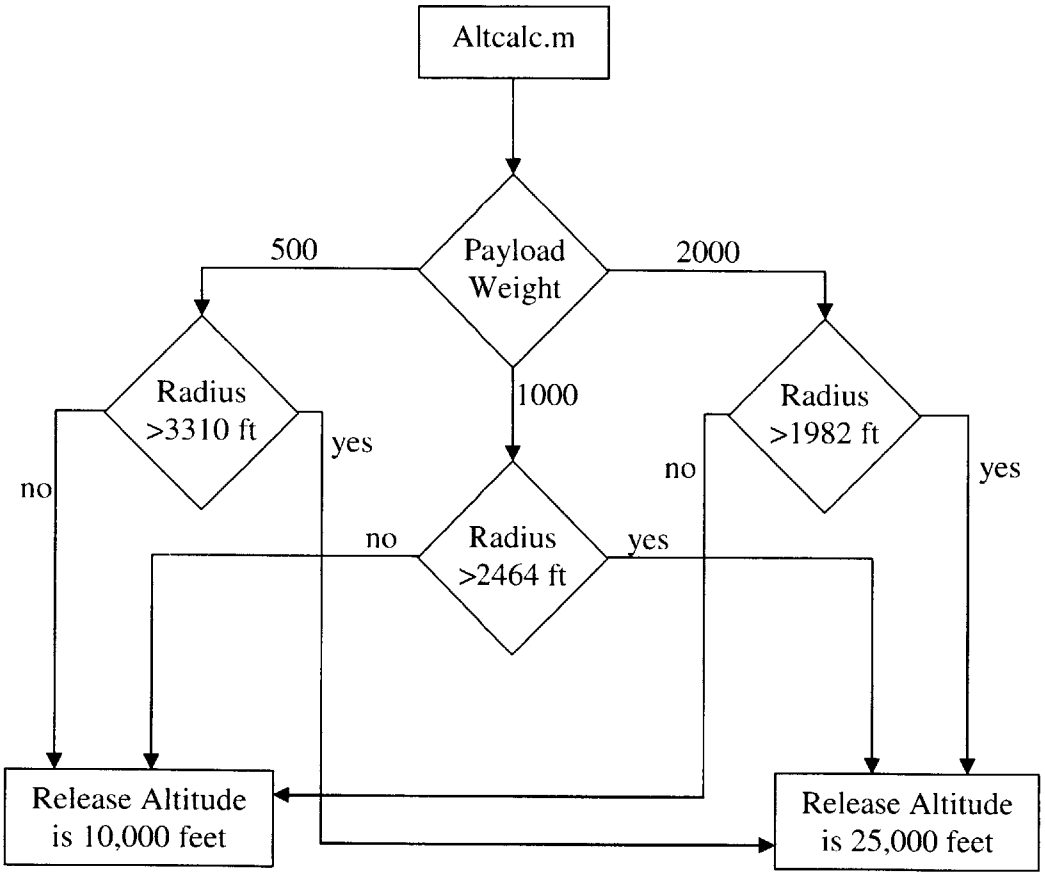

Figure 5.2. Altcalc.m Decision Process for an Unguided System

Examples of altcalc.m in use are shown below:

```
>> altcalc
Enter payload weight in pounds (500, 1000, or 2000 pounds)1000
Enter maximum desired landing area radius in feet (no less than 1795 feet)3000

Adequate release altitude is 25,000 feet

>> altcalc
Enter payload weight in pounds (500, 1000, or 2000 pounds)2000
Enter maximum desired landing area radius in feet (no less than 1474 feet)1600

Adequate release altitude is 10,000 feet
```

Figure 5.3. Determining an Adequate Release Altitude for an Unguided System

Another script was written in Matlab, named radiuscalc.m, to determine the required landing area radius for a given situation. This is basically the inverse to altcalc.m, and it is the equivalent of simply looking at Table 5.1. Its use is shown here:

```
>> radiuscalc
Enter guidance option (1 = guided, 0 = unguided)0
Enter payload weight in pounds (500, 1000, or 2000 pounds)500
Enter release altitude in feet (10,000 or 25,000 feet)25000

Required landing area radius is approximately 3311 feet

>> radiuscalc
Enter guidance option (1 = guided, 0 = unguided)0
Enter payload weight in pounds (500, 1000, or 2000 pounds)1000
Enter release altitude in feet (10,000 or 25,000 feet)10000

Required landing area radius is approximately 1795 feet
```

Figure 5.4. Determining the Required Landing Area Radius for an Unguided System

Due to the limited number of scenarios studied, there is currently not enough data to use these tools for other release altitudes and payload weights. However, with more data points, these types of tool can be very useful when planning an airdrop. Not only will

there be more release altitudes and payloads to choose from, but with more data points, landing errors for altitudes and payloads not simulated can be more easily estimated.

5.4 Guided Airdrop Planning Aid

For the unguided system, different scenarios could mean differences of hundreds of feet in the required landing area radii. The differences are not so drastic for the guided system, where the highest required landing area radius is 344 feet. After it has been decided to use the guided system, it is then time to determine what type of wind knowledge will be used, and also to decide if any onboard wind measurement devices will be used.

It was shown in Chapter 4 that not using any wind knowledge at all is a perfectly valid choice for guided systems, as the performance is approximately equal to, if not better than, the performance of the other wind knowledge choices. That can also be seen in Table 5.2. It was also previously determined that not using any wind knowledge can be unfavorable if there are heavy winds. One way to solve this problem is to use a balloon or dropsonde to measure the winds, and if the winds are measured to be strong, use the forecasted data. Otherwise, disregard the forecasted data and drop the parafoil as if there was no wind knowledge.

Another way to reduce errors, and thus reduce the required landing area radius, is to use an onboard wind measurement system. Looking at Table 5.2, using onboard sampling reduces some of the larger errors, while look-ahead sampling noticeably reduces all of the errors for a given wind knowledge. Using look-ahead sampling for any type of wind knowledge will give a required landing area radius of less than 80 feet.

It can be deduced from Table 5.2 that using general statistics as a means for estimating wind has no actual benefit when using a guided system. Not using any wind knowledge will perform just as well, if not better. Also, the only reason to use balloon forecasting as a means for estimating wind is to determine how strong the winds are. Only if the winds

are considered to be strong, relative to the parafoil's horizontal airspeed, will it be beneficial to use the forecasted data.

Similar to the unguided air release planning tools shown above, Matlab scripts were written for the guided system to assist in airdrop planning. The first script, samplingcalc.m, determines what type of sampling method to use to ensure a landing within a desired landing area radius. The decision process for samplingcalc.m is shown here in Figure 5.5. Diamond shapes represent decisions and rectangles represent actions.

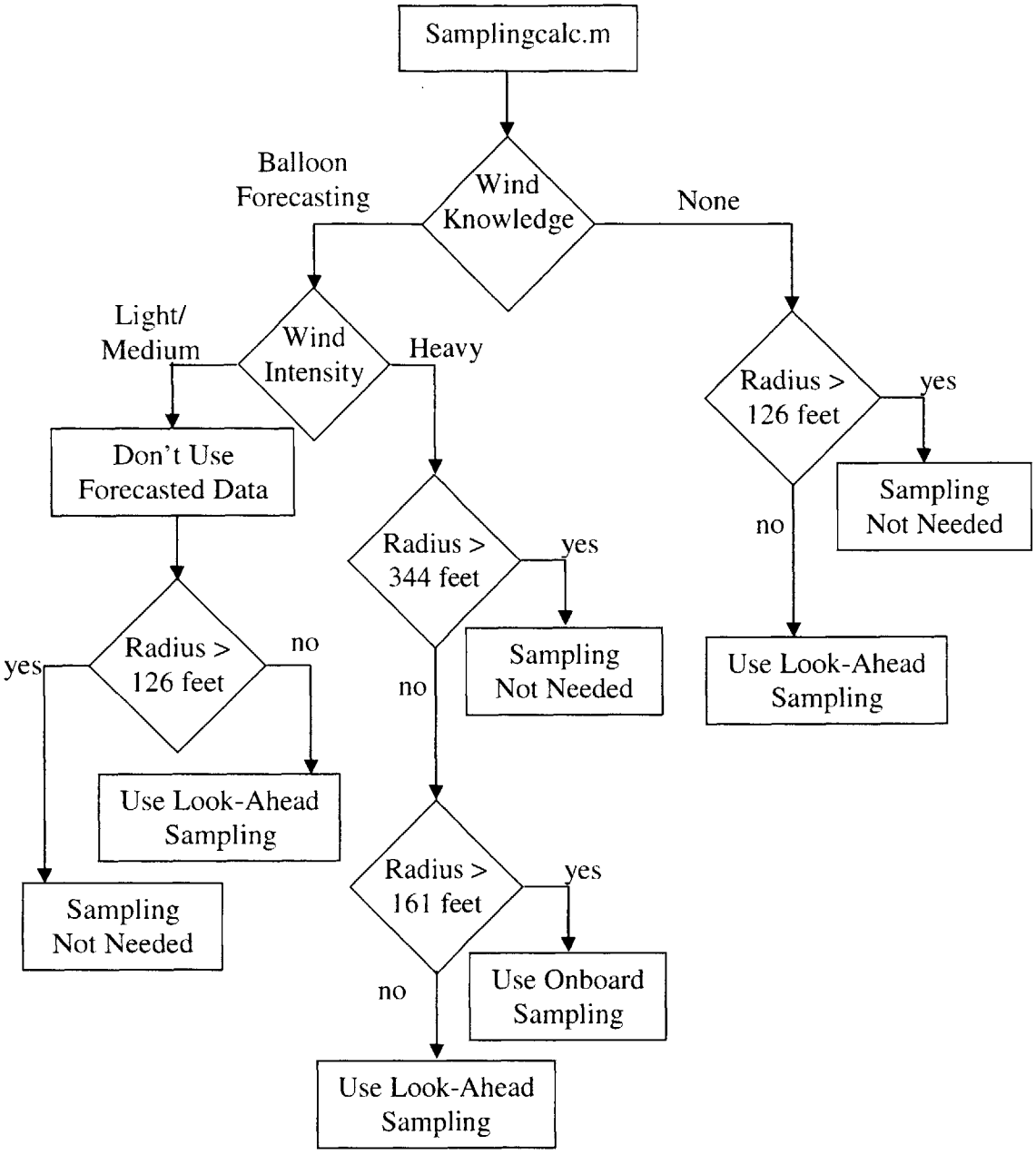

Figure 5.5. Samplingcalc.m Decision Process

Examples of samplingcalc.m in use are shown in Figure 5.6:

```
>> samplingcalc
Enter maximum desired landing area radius in feet (no less than 80 feet)100
Enter wind knowledge (0 = no wind knowledge, 1 = balloon forecasting)1
Enter wind intensity (0 = low/medium winds, 1 = high winds)0

Do not use any forecasted wind for this airdrop
Adequate sampling method is: look-ahead sampling

>> samplingcalc
Enter maximum desired landing area radius in feet (no less than 80 feet)300
Enter wind knowledge (0 = no wind knowledge, 1 = balloon forecasting)1
Enter wind intensity (0 = low/medium winds, 1 = high winds)1

Adequate sampling method is: current wind
```

Figure 5.6. Determining Adequate Wind Knowledge Requirements for a Guided System

As with the unguided air release planning system, radiuscalc.m can also be used with the guided airdrop system to determine the required landing area radius, as shown here:

```
>> radiuscalc
Enter guidance option (1 = guided, 0 = unguided)1
Enter wind knowledge (0 = no wind knowledge, 1 = balloon forecasting)0
Enter sampling method (0 = none, 1 = current wind, 2 = wind below)1

Required landing area radius is approximately 158 feet

>> radiuscalc
Enter guidance option (1 = guided, 0 = unguided)1
Enter wind knowledge (0 = no wind knowledge, 1 = balloon forecasting)1
Enter sampling method (0 = none, 1 = current wind, 2 = wind below)2
Enter wind intensity (0 = low/medium winds, 1 = high winds)1

Required landing area radius is approximately 80 feet
```

Figure 5.7. Determining the Required Landing Area Radius for a Guided System

Another benefit of using guidance during an airdrop is that the parafoil does not have to be released at the CARP (computed aerial release position). The region that defines where the parafoil can be released from and still make it to the target is known as the

drop basket. Using its guidance, the parafoil can usually make it towards the target as long as the release point is in this basket, and this basket allows the parafoil to reach the target area with some reserve altitude for precision landing. As the release point approaches and surpasses the drop basket radius, landing errors will begin to increase. Figure 5.8, shown below, displays the effect of release position error on landing accuracy.

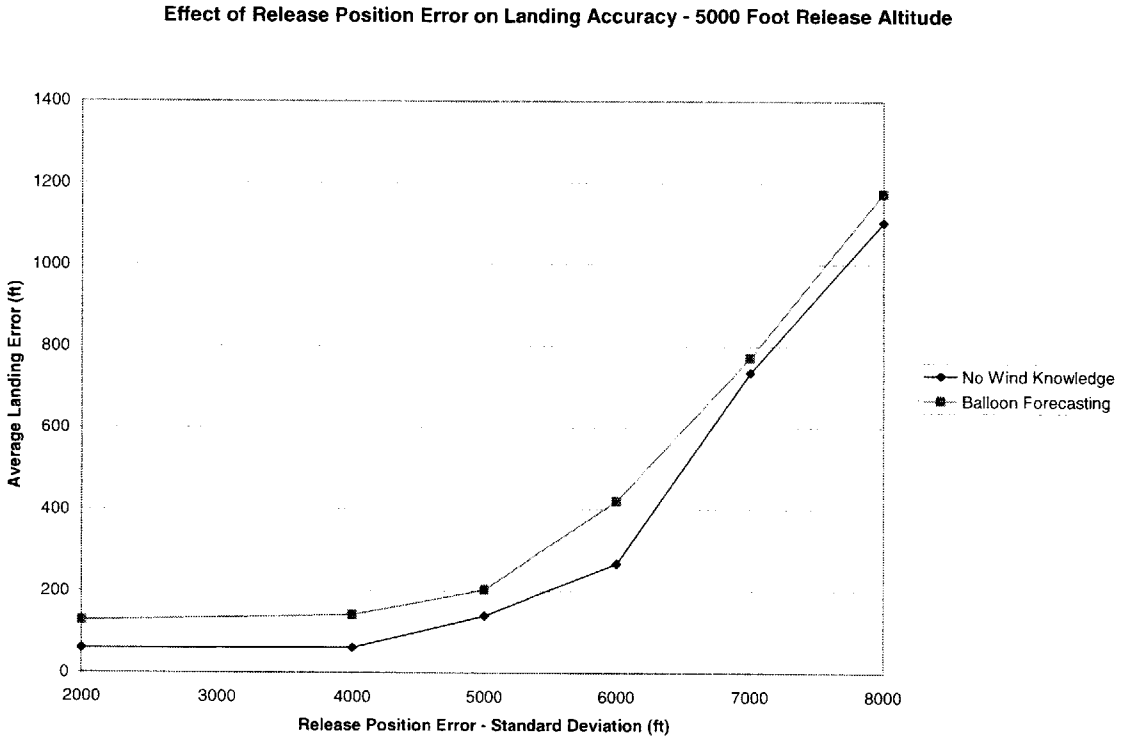

Figure 5.8. Effect of Release Position Error on Landing Accuracy

In Figure 5.8, 200-run Monte Carlo simulations were performed. For these simulations, the release position error in both the North-South direction and the East-West direction was considered Gaussian with zero mean and a particular standard deviation. The plot shows that as the standard deviation approached the release altitude distance, errors began to develop. This in turn implies that the drop basket has a radius similar to the release altitude. As long as the parafoil is released within this radius, it should be able to reach the target. This result is not accurate for all parafoils however. The drop basket radius is highly dependent on the lift-to-drag ratio of the parafoil. The greater the lift-to-

drag ratio, the further the horizontal distance is that the parafoil can travel, thus increasing the drop basket radius.

5.5 Enhancing the Airdrop Planning Aid

The airdrop planning aid described in this chapter outlines a procedure that can be used as a template for a more detailed airdrop planning aid. The planning aid shown here is only valid for the PADS and PGAS systems that were studied. Practical planning aids will be tailored to the types of systems being used, if they are different.

One method of enhancing the airdrop planning aid is to develop physics-based models to aid in the extrapolation and interpolation of data from, and between related, airdrop systems. This task is not trivial, as airdrops have many random components and are non-linear. However, estimated formulas can help to improve the estimation of landing accuracy for scenarios that haven't been simulated.

Adding more data points to the unguided air release planning system study will greatly enhance the capabilities of this planner. Landing errors were found to be a function of release condition errors, parachute dynamics errors, and wind estimation errors. These errors developed differently for different scenarios.

Simulating more errors in a guided airdrop system will also enhance the capabilities of this planner. Some possibilities include release condition errors and sensor errors. It is often assumed that release conditions errors are small enough that the parafoil reaches the steady-state flight mode within the drop basket. There may be some cases where this is not always true. For example, if the parafoil opens at a relatively low altitude, release condition errors could play a factor in getting the payload to the target. Implementing a simulation that accurately adjusts for sensor errors will also provide for more meaningful results, as sensor errors are believed to play a role in guided system landing accuracy.

For both unguided and guided systems, more landing errors can be generated to improve the capabilities of the airdrop planning aid. When implementing these errors in a simulation, landing errors should be generated for scenarios defined by four criteria: parachute type, payload weight, release altitude, and wind estimation system. Depending on the wind estimation system, wind intensity could be a fifth criterion. With more data points, not only will there be more situations to choose from, but landing errors for scenarios not simulated can be more easily estimated.

5.6 Conclusions

When determining the best method to perform an airdrop, the first decision should be whether or not to use guidance. It is beneficial to determine what kind of accuracy is required since the differences in landing errors (and thus required landing area radii) are great between unguided and guided systems. Using guidance can drastically improve landing accuracy.

If using an unguided air release planning system to perform an airdrop, the expected landing errors will depend on many factors. The airdrop personnel can reduce the expected landing error by increasing the payload weight, reducing the release altitude, and using a more accurate wind estimation system. For guided systems, the best way to reduce errors is to have an onboard wind measurement system to update the predicted wind profile of the guided parafoil. Also for guided systems, the parafoil does not have to be released at the exact CARP. It can be released anywhere in the drop basket, and still land near the target.

The airdrop planning aid described in this chapter can be used as a template for developing a more practical and more reliable airdrop planning aid. More data points and more accurate error representations of guided systems are necessary to create this practical airdrop planning aid.

Chapter 6
Conclusions and Recommendations

6.1 Conclusions

This project attempted to provide information in the pursuit of improving airdrop accuracy, for both unguided air release planning systems and guided airdrop systems. Major sources of landing error for airdrops were derived and analyzed. Expected landing errors were also determined for various airdrop scenarios.

It was found that the major source of landing error for both unguided and guided systems is error in wind knowledge. For unguided systems, the longer the parachute is in the air, the greater the landing error will be due to wind knowledge error. For guided systems, the wind knowledge error has the greatest effect near the ground, as the target is incorrectly offset to account for the predicted wind. Also for guided systems, the wind knowledge error can be reduced in-flight with use of onboard wind measurement systems. Developing better wind estimation systems will certainly improve landing accuracy in all situations.

In many situations, it was found that not using any wind knowledge for the guided system outperformed the drops that used some form of wind prediction. The parafoil was able to maneuver through the wind and remain close to the target without offsetting the target due to a predicted wind profile.

Required landing area radii were calculated to ensure safe delivery within a landing area, taking into account all the errors studied. It was shown that the use of guidance in airdrops outperformed unguided systems by a large margin. The required landing area radii for unguided systems were calculated to be approximately between 1500 and 3500 feet, whereas the range for guided systems was calculated to be approximately between 75 and 350 feet.

6.2 Thesis Summary

Several wind prediction methods were analyzed and modeled to better understand the effects of wind on airdrop systems. It was shown that wind estimation errors were best described in terms of errors in the North and East directions, as these errors are Gaussian and thus mathematically easier to implement in the simulations. The data also showed that the magnitude of the actual wind had little relation to the magnitude of the wind prediction error. The correlations of these wind errors with respect to altitude difference were assessed. Methods for incorporating onboard wind measurement into the wind prediction were also discussed and implemented.

Error analysis was performed on an unguided air release planning system with a simulation known as PADS, or Precision Aerial Delivery System. It was shown that errors in wind prediction produced more landing error than any other error source. Errors in exit time upon release were the second greatest cause of error. Monte Carlo simulations were executed to determine the expected landing errors for 18 different unguided scenarios. Wind intensity was found to have no effect on landing error, while both an increase in release altitude and a decrease in payload weight were shown to increase landing error. The reason that these two changes increase landing error is due to the fact that the payload is in the air for a longer period of time, and the wind has more time to move the parachute further from the target. Sensitivities of component errors were also examined, and it was found that six out of seven of the component errors had an approximately linear relation to their effective landing errors.

Error analysis was performed on a guided airdrop system with a simulation known as PGAS, or Precision Guided Airdrop System. Monte Carlo simulations were executed for various scenarios. It was shown for guided systems that both release altitude and payload weight had negligible or no effect on the landing error. For the simulations that used a priori wind knowledge, the parafoil's target was offset with relation to the predicted wind. It was shown that using no wind knowledge is just as effective, if not better, than using a wind prediction to offset the target. The exception is when the wind is very strong in relation to the parafoil's horizontal airspeed. In this case, the parafoil can not struggle though the wind and using a wind-offset target will be advantageous. It was also shown that using onboard wind measurement systems are a valuable tool in reducing landing error, with the landing error decreasing the further ahead the wind measurements are taken.

The data from both the unguided and guided systems were combined to form a tool to assist in airdrop planning. The tool developed in this study is not a complete product, but represents a template for developing a practical airdrop planning aid. The tool was designed to aid in two separate ways. First, the required landing area radius can be calculated for a given set of airdrop properties. Second, the tool can determine what types of adjustments can be made to achieve a desired landing accuracy.

6.3 Recommendations

As wind has shown to be a major factor in airdrop landing accuracy, more in-depth research into wind characteristics will be valuable to accuracy studies. More data from balloon forecasting will provide more accurate representations of the forecasting errors and the resulting altitude-dependent error correlations. Other methods of wind predicting can also be analyzed and tailored to various geographic locations where airdrops are expected to be executed. Also, vertical components of winds can be examined to determine the effects on airdrop accuracy; however the vertical wind data is often not readily available.

For unguided air release planning systems, performing more Monte Carlo simulations for more scenarios will be useful in determining the exact relation that components such as payload weight and release altitude have on landing accuracy. Due to the complex non-linearity of an airdrop, physics-based models are difficult to develop when attempting to determine these relations. Therefore, more data will be helpful, as various curve-fitting techniques can be implemented. Also, using different-sized parachutes in simulations could show how the different parachute dynamics affect landing accuracy.

For guided airdrop systems, additional guidance algorithms can be used in simulation to compare with the simulation used in this study. It will also be beneficial to study guided airdrop systems by attempting to always land the parafoil into the predicted wind, as is done in actual guided airdrops. Wind knowledge will have an effect on this type of landing process, and it may be helpful to determine the relation between wind knowledge and the ability to land into the wind. Wind direction had no affect on the choice of landing heading in this study. It will also be advantageous to analyze the landing accuracies for larger parafoils than the 88 square foot parafoil used in this study. Different dynamics for larger parafoils could provide different results.

Incorporating the use of terrain models into airdrop systems is another recommended continuation of this study. When the required landing area size has been calculated, a system can then use a terrain model to determine adequate landing targets. This will provide for more flexibility in landing locations.

As mentioned above, more data would be beneficial to develop a useful tool for airdrop planning. The tool that was developed here uses only the results from this study. Expanding this study to include other simulations, types of parachutes, release altitudes, and so on will provide for a more reliable and practical airdrop planning tool.

References

[1] Hattis, P., Fill, T., Rubenstein, D., Wright, R., Benney, R., and Lemoine, D., "Status of an On-Board Airdrop Planner Demonstration," AIAA Paper 2001-2066, 2001.

[2] Hattis, P. D., Appleby, B. D., and Fill, T. J., "Precision Guided Airdrop System Flight Test Results," AIAA Paper, 1997.

[3] Hattis, P. D., Fill, T. J., Rubenstein, D. S., Wright, R. P., and Benney, R. J., "An Advanced On-Board Airdrop Planner to Facilitate Precision Payload Delivery," AIAA Paper 2000-4307, 2000.

[4] Justus, C. G., Jeffries III, W. R., Yung, S. P., and Johnson, D. L., "The NASA/MSFC Global Reference Atmospheric Model – 1995 Version (GRAM-95)," NASA Technical Memorandum 4715, August 1995.

[5] Wijting, C., Braia, E., Cianca, E., and Prasad, R., "Error Control Mechanisms Over Correlated Fading Channels," IEEE Paper 0-7803-7589-0/02, 2002.